

Bulletin 97

New Mexico Museum of Natural History & Science

A Division of the

DEPARTMENT OF CULTURAL AFFAIRS

**EARLY DIENERIAN AMMONOIDS AND NAUTILOIDS
AND A NEW LATE GRIESBACHIAN AMMONOID SITE
FROM THE DINWOODY FORMATION (THAYNES
GROUP) AT CRITTENDEN SPRINGS, ELKO COUNTY,
NEVADA**

by

**JAMES F. JENKS, TAKUMI MAEKAWA, YASUNARI
SHIGETA, DAVID WARE, ARNAUD BRAYARD, KEVIN
G. BYLUND, DANIEL A. STEPHEN AND NOREEN
KITTRICK**

New Mexico Museum of Natural History & Science

Albuquerque, 2025

STATE OF NEW MEXICO
Department of Cultural Affairs
Debra Garcia y Griego, *Secretary*

NEW MEXICO MUSEUM OF NATURAL HISTORY AND SCIENCE
Anthony R. Fiorillo Ph.D, *Executive Director*

BOARD OF TRUSTEES

Michelle Lujan Grisham, Governor, State of New Mexico, *ex officio*

Anthony R. Fiorillo Ph.D, *Executive Director*

Gary Friedman, *President*

Laura Smigielski Garcia, *Secretary*

James Bryant

Dr. Sara Fuentes-Soriano

Isatu Kaigziabiher

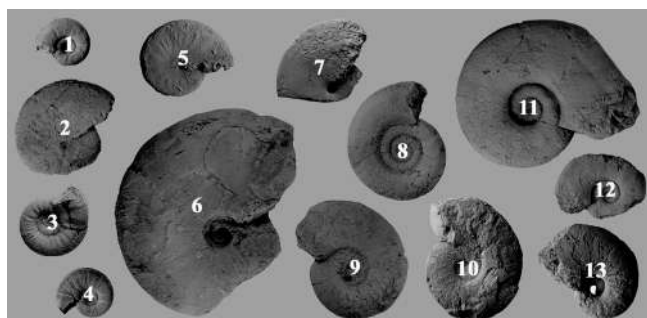
Dr. Barry S. Kues

Antonio Lopez

Rob Nelson

Ian Noble

Robert Vladem



Cover illustration: Cover illustration: Crittenden Springs Early Triassic (early Dienerian and late Griesbachian) ammonoids and nautiloids: 1-*Gyronites rigidus* (Diener), 2-*Ghazalaites roohiae* Ware and Bucher, 3-*Gyronites rigidus* (Diener), 4-*Gyronites rigidus* (Diener), 5-*Ussuridiscus varaha* (Diener), 6-*Ussuridiscus varaha* (Diener), 7-*Ussuridiscus varaha* (Diener), 8-*Gyronites frequens* Waagen, 9-*Gyronites frequens* Waagen, 10-*Gyronites frequens* Waagen, 11-*Wordieoceras wordiei* (Spath), 12-*Wordieoceras wordiei* (Spath), 13-*Xiaohenautilus chatelaini* n. sp.

Associate editor for this bulletin: Spencer G. Lucas

Original Printing

ISSN: 1524-4156

Available from the New Mexico Museum of Natural History and Science,
1801 Mountain Road NW, Albuquerque, NM 87104; Telephone (505) 841-2800;
Fax (505) 841-2866; www.nmnaturalhistory.org

NMMNH Bulletins online at: <http://nmnaturalhistory.org/bulletins> and Google Books

**BULLETIN OF THE NEW MEXICO MUSEUM
OF NATURAL HISTORY AND SCIENCE**

EDITORS

Spencer G. Lucas	New Mexico Museum of Natural History and Science, Albuquerque, NM, USA (NMMNHS)
Adrian P. Hunt	Flying Heritage Collection, Everett, WA, USA
Jason L. Malaney	NMMNHS
Lawrence H. Tanner	Le Moyne College, Syracuse, NY, USA

MANAGING EDITOR

Asher J. Lichtig	NMMNHS
-------------------------	--------

ASSOCIATE EDITORS

Guillermo Alvarado	Asociación Costarricense de Geotecnica, San José, Costa Rica
Marco Avanzini	Museo Tridentino di Scienze Naturali, Trento, Italy
David Berman	Carnegie Museum of Natural History, Pittsburgh, PA, USA
Brent Breithaupt	US Bureau of Land Management, Laramie, WY, USA
William DiMichele	National Museum of Natural History, Washington, D.C., USA
John R. Foster	Utah Field House of Natural History State Park Museum, Vernal, UT, USA
Gerard Gierlinski	Polish Geological Institute, Warsaw, Poland
Jean Guex	University of Lausanne, Lausanne, Switzerland
Steven E. Jasinski	Harrisburg University, Harrisburg, PA, USA
Hendrik Klein	Neumarkt, Germany
Karl Krainer	University of Innsbruck, Innsbruck, Austria
Gary S. Morgan	NMMNHS
Donald R. Prothero	State Polytechnic University Pomona, CA, USA
Silvio Renesto	Università degli Studi dell'Insubria, Varese, Italy
Joerg W. Schneider	Technical University BergAkademie of Freiberg, Freiberg, Germany
Jingeng Sha	Nanjing Institute of Geology and Palaeontology, Nanjing, China
Dana Ulmer-Scholle	NM Bureau of Geology & Mineral Resources, Socorro, NM, USA
Sebastian Voigt	Urweltmuseum GEOSKOP/Burg Lichtenburg, Thallichtenberg, Germany
Ralf Werneburg	Naturhistorisches Museum Schloss Bertholdsburg, Schleusingen, Germany
Richard S. White, Jr.	Mammoth Site, Hot Springs, SD, USA

55. Tetrapod fauna of the Upper Triassic Redonda Formation, east-central New Mexico: The characteristic assemblage of the Apachean land-vertebrate faunachron, 2012, by Justin A. Spielmann and Spencer G. Lucas, 119 pp.
56. Revision of the Lower Triassic tetrapod ichnofauna from Wióry, Holy Cross Mountains, Poland, 2012, by Hendrik Klein and Grzegorz Niedzwiedzki, 62 pp.
57. Vertebrate Coprolites, 2012, edited by Adrian P. Hunt, Jesper Milàn, Spencer G. Lucas and Justin A. Spielmann, 387 pp.
58. A new archaic basking shark (Lamniformes: Cetorhinidae) from the late Eocene of western Oregon, U.S.A., and description of the dentition, gill rakers and vertebrae of the recent basking shark *Cetorhinus maximus* (Gunnerus), 2013, by Bruce J. Welton, 48 pp.
59. The Carboniferous-Permian transition in central New Mexico, 2013, edited by Spencer G. Lucas, W. John Nelson, William A. DiMichele, Justin A. Spielmann, Karl Krainer, James E. Barrick, Scott Elrick and Sebastian Voigt, 389 pp.
60. The Carboniferous-Permian transition, 2013, edited by Spencer G. Lucas, William A. DiMichele, James E. Barrick, Joerg W. Schneider and Justin A. Spielmann, 465 pp.
61. The Triassic System: New Developments in Stratigraphy and Paleontology, 2013, edited by Lawrence H. Tanner, Justin A. Spielmann and Spencer G. Lucas, 612 pp.
62. Fossil Footprints of Western North America, 2014, edited by Martin G. Lockley and Spencer G. Lucas, 508 pp.
63. Variation in the Dentition of *Coelophysis bauri*, 2014, by Lisa G. Buckley and Philip J. Currie, 73 pp.
64. Conodonts from the Carnian-Norian Boundary (Upper Triassic) of Black Bear Ridge, Northeastern British Columbia, Canada, 2014, by Michael J. Orchard, 139 pp.
65. Carboniferous-Permian Transition in the Robledo Mountains Southern New Mexico, 2015, edited by Spencer G. Lucas and William A. DiMichele, 167 pp.
66. The Marine Fish Fauna of the Middle Pleistocene Port Orford Formation and Elk River Beds, Cape Blanco, Oregon, 2015, by Bruce J. Welton, 45 pp.
67. Fossil Record 4, 2015, edited by Robert M. Sullivan and Spencer G. Lucas, 332 pp.
68. Fossil Vertebrates in New Mexico, 2015, edited by Spencer G. Lucas and Robert M. Sullivan, 438 pp.
69. The Pennsylvanian System in the Mud Springs Mountains, Sierra County, New Mexico, USA, 2016, by Spencer G. Lucas, Karl Krainer, James E. Barrick and Daniel Vachard, 58 pp.
70. *Eocyclotosaurus appetolatus*, a Middle Triassic Amphibian, 2016, by Rinehart and Lucas, 118 pp.
71. Cretaceous Period: Biotic Diversity and Biogeography, 2016, edited by Khosla and Lucas, 330 pp.
72. Rotten Hill: a Late Triassic Bonebed in the Texas Panhandle, USA, 2016, by S.G. Lucas, L.F. Rinehart, A.B. Heckert, A.P. Hunt and J.A. Spielmann, 97 pp.
73. The Red Corral (Proctor Ranch) Local Fauna (Pliocene, Blancan) of Oldham County, Texas, 2016, by G.E. Schultz,
74. Fossil Record 5, 2016, edited by Robert M. Sullivan and Spencer G. Lucas, 352 pp.
75. New Well Peak, 2017, by Karl Krainer, Daniel Vachard and Spencer G. Lucas, 163 pp.
76. The Locketong Formation, 2017, by David L. Fillmore, Michael J. Szajna, Spencer G. Lucas, Brian W. Hartline and Edward L. Simpson, 107 pp.
77. Carboniferous-Permian transition in Socorro County, New Mexico, 2017, edited by Spencer G. Lucas, William A. DiMichele and Karl Krainer, 352 pp.
78. Smithian (Early Triassic) Ammonoids from Crittenden Springs, 2018, James F. Jenks and Arnaud Brayard, 175 pp.
79. Fossil Record 6, 2018, edited by Spencer G. Lucas and Robert M. Sullivan, 768 pp.
80. Late Cretaceous Ammonites from the Southeastern San Juan Basin, 2019, Paul L. Sealey and Spencer G. Lucas, 245 pp.
81. Stratigraphic, Geographic and paleoecological distribution of the Late Cretaceous shark genus *Ptychodus* within the Western Interior Seaway, North America, 2020, Shawn A. Hamm, 94 pp.
82. Fossil Record 7, 2021, edited by Spencer G. Lucas, Adrian P. Hunt and Asher J. Lichtig, 578 pp.
83. The Triassic Tetrapod Footprint Record, 2021, Hendrik Klein and Spencer G. Lucas, 194 pp.
84. Kinney Brick Quarry Lagerstätte, 2021, edited by Spencer G. Lucas, William A. DiMichele and Bruce D. Allen, 468 pp.
85. The Systematics of North American Peccaries, 2021, Donald R. Prothero, 76 pp.
86. Late Griesbachian, Dinwoody Formation, Ammonoids and Nautiloids, 2021, James F. Jenks, Takumi Maekawa, David Ware, Yasunari Shigeta, Arnaud Brayard and Kevin G. Bylund, 23 pp.
87. The Ichnology Of Vertebrate Consumption, 2021, Adrian P. Hunt and Spencer G. Lucas, 216 pp.
88. Late Cenozoic Vertebrate Paleontology: Tribute to Arthur H. Harris, 2022, edited by Gary S. Morgan, Jon A. Baskin, Nicholas J. Czaplewski, Spencer G. Lucas, H. Gregory McDonald, Jim I. Mead, Richard S. White, Jr., and Asher J. Lichtig, 370 pp.
89. The Pennsylvanian Section At Bishop Cap And The Horquilla Seaway In The Southwestern USA-Northern Mexico, Spencer G. Lucas, Karl Krainer, Daniel Vachard and James E. Barrick, 77 pp.
90. Fossil Record 8, 2022, Edited by Spencer G. Lucas, Robert B. Blodgett, Asher J. Lichtig and Adrian P. Hunt, 495 pp.
91. Ammonites From the Pierre Shale, 2022, Paul L. Sealy and Spencer G. Lucas, 183 pp.
92. Geology of the Mud Springs Mountains 2023, Spencer G. Lucas, Karl Krainer, James E. Barrick, Daniel Vachard, Chelsea F. Ottenfeld and Jeffrey M. Amato, 92 pp.
93. Systematics of the Late Oligocene and Miocene Oreodonts 2023, Margaret Skeels Stevens, Donald R. Prothero, Casey Cleaveland, Ed Welsh, Katherine Marriott, Thein Htun, Daniella Balassa, Sara M. Olson, Kristin I. Watmore and Dacia Wheeler, 226 pp.
94. Fossil Record 9, 2023, Edited by Spencer G. Lucas, Asher J. Lichtig, Gary S. Morgan and Adrian P. Hunt, 708 pp.
95. Vertebrate Paleoichnology: A Tribute to Martin Lockley, 2024, Louis H. Taylor, Robert G. Reynolds, and Spencer G. Lucas, 438 pp.
96. Lamy Amphibian Quarry, A Late Triassic Metoposaur-Dominated Bonebed In New Mexico, 2024, Larry F. Rinehart, Spencer G. Lucas and Andrew B. Heckert, 154 pp.

**EARLY DIENERIAN AMMONOIDS AND NAUTILOIDS AND A NEW
LATE GRIESBACHIAN AMMONOID SITE FROM THE DINWOODY
FORMATION (THAYNES GROUP) AT CRITTENDEN SPRINGS, ELKO
COUNTY, NEVADA**

JAMES F. JENKS, TAKUMI MAEKAWA, YASUNARI SHIGETA, DAVID WARE, ARNAUD
BRAYARD, KEVIN G. BYLUND, DANIEL A. STEPHEN and NOREEN KITTRICK

Contents

INTRODUCTION.....	1
LOCALITY AND GEOLOGICAL CONTEXT.....	4
Location.....	4
Dinwoody Formation.....	4
Lithostratigraphic Divisions.....	5
Study Area Outcrops.....	6
Descriptions of Newly Found Early Dienerian and Late Griesbachian Ammonoid Sites.....	6
Early Dienerian Ammonoid and Nautiloid Site.....	6
New Late Griesbachian Ammonoid Site.....	6
DIENERIAN AMMONOID BIOSTRATIGRAPHY.....	8
NORTH AMERICA.....	8
BOREAL REALM	8
NORTHERN INDIAN MARGIN.....	9
SOUTH CHINA.....	9
SOUTH PRIMORYE.....	10
IRAN.....	10
THE BASAL DIENERIAN INDEX CONODONT SWEETOSPATHODUS KUMMELI AND THE GRIESBACHIAN/DIENERIAN BOUNDARY (GDB)	10
SYSTEMATIC PALEONTOLOGY.....	10
Class CEPHALOPODA Cuvier, 1797.....	11
Superorder AMMONOIDA Hoffmann, 2022.....	11
Order CERATITIDA Hyatt, 1884.....	11
Superfamily MEEKOCERATOIDEA Waagen, 1895.....	11
Family OPHICERATIDAE Arthaber, 1911.....	11
Genus <i>Ghazalaites</i> Ware and Bucher, 2018a.....	11
Family GYRONITIDAE Waagen, 1895.....	11
Genus <i>Gyronites</i> Waagen, 1895.....	11
Family PROPTYCHITIDAE Waagen, 1895.....	15
Genus <i>Proptychites</i> Waagen, 1895.....	15

Family MULLERICERATIDAE Ware et al., 2011.....	17
Genus <i>Ussuridiscus</i> Shigeta and Zakharov, 2009.....	17
Family OPHICERATIDAE Arthaber, 1911.....	19
Genus <i>Wordieoceras</i> Tozer, 1971.....	19
Family INCERTAE SEDIS.....	21
Order NAUTILIDA Agassiz, 1847.....	23
Superfamily TRIGONOCERATOIDEA Hyatt, 1884.....	23
Family GRYPOCERATIDAE Hyatt, 1900.....	23
Genus <i>Xiaohenautilus</i> Xu, 1988.....	23
CONCLUSIONS.....	23
ACKNOWLEDGMENTS.....	23
AUTHOR CONTRIBUTIONS.....	26
REFERENCES.....	26
APPENDIX.....	29

EARLY DIENERIAN AMMONOIDS AND NAUTILOIDS AND A NEW LATE GRIESBACHIAN AMMONOID SITE FROM THE DINWOODY FORMATION (THAYNES GROUP) AT CRITTENDEN SPRINGS, ELKO COUNTY, NEVADA

JAMES F. JENKS¹, TAKUMI MAEKAWA², YASUNARI SHIGETA³, DAVID WARE⁴, ARNAUD BRAYARD⁵, KEVIN G. BYLUND⁶, DANIEL A. STEPHEN⁷ AND NOREEN KITTRICK⁸

¹1134 Johnson Ridge Lane, West Jordan, UT 84084, e-mail: Jim42ryjenks@comcast.net; ²Osaka Museum of Natural History, 1-23 Nagai Park, Higashi-sumiyoshi-ku, Osaka 546-0034, Japan, e-mail: t.m.127d@gmail.com; ³Department of Geology and Paleontology, National Museum of Nature and Science, 4-1-1 Amakubo, Tsukuba, Ibaraki 305-0005, Japan, e-mail: shigeta@kahaku.go.jp; ⁴Museum für Naturkunde, Leibniz Institute for Evolution and Biodiversity Science, Invalidenstrasse 43, 10115 Berlin, Germany, e-mail: david.ware@mfn.berlin; ⁵Biogéosciences, UMR 6282 CNRS, Université de Bourgogne, 21000 Dijon, France, e-mail: arnaud.brayard@u-bourgogne.fr; ⁶140 South 700 East, Spanish Fork, UT 84660; e-mail: kgbylund@gmail.com; ⁷Department of Earth Sciences, Utah Valley University, 800 W. University Parkway, Orem, Utah 84058, e-mail: daniel.stephen@uvu.edu; ⁸347 E Blaine Ave, Salt Lake City, Utah 84115, e-mail: nkittrick@gmail.com

Abstract—Ongoing exploration in the Dinwoody Formation of the Thaynes Group at Crittenden Springs, Elko County, Nevada, motivated by the earlier reported discovery of late Griesbachian ammonoids and nautiloids, has led to the discovery of an early Dienerian ammonoid and nautiloid assemblage as well as a new late Griesbachian ammonoid site. The early Dienerian ammonoid fauna includes the genus *Gyronites*, heretofore known only from the Tethys and South Primorye, and the Crittenden Springs assemblage represents the only low-paleolatitude early Dienerian ammonoid and nautiloid occurrence in eastern Panthalassa. Early Dienerian ammonoid taxa include *Gyronites rigidus* (Diener), *Gy. frequens* Waagen, *Gy. bullatus* Ware and Bucher, *Ussuridiscus varaha* (Diener), *Ghazalaites roohiae* Ware and Bucher, *Proptychites* sp. and gen. et sp. indet. This assemblage correlates broadly with the early Dienerian of the Northern Indian Margin (NIM: Salt Range, Pakistan, Spiti, Himalaya and South Tibet, China). Nautiloids include *Xiaohenautilus mulleni* Jenks et al. and a new taxon, i.e., *Xiaohenautilus chatelaini* n. sp. The new late Griesbachian ammonoid site has yielded *Wordieceras wordiei* (Spath) and *W. mullenae* Jenks et al. Several early Dienerian and late Griesbachian conodont taxa, including *Sweetospathodus kummeli*, the conventional basal Dienerian index marker, have been recovered from the study area. However, the validity of this taxon as a marker for the G/D boundary is questioned because of its first occurrence (FO) ~30 m above the FO of basal early Dienerian ammonoids.

INTRODUCTION

According to some workers (Hallam, 1991; Tong et al., 2007; Chen and Benton, 2012), the recovery of marine life following the Permian-Triassic (PT) mass extinction ~252 million years ago, which is estimated to have wiped out nearly 90% of all marine species (Raup, 1979; Stanley, 2016), was delayed at least until Middle Triassic time for many clades. Until recently, the oldest known Triassic complex marine ecosystem was the Anisian-age Luoping biota of South China (Hu et al., 2011). However, extensive fieldwork over the past 15 years has shown that many groups, e.g., the ammonoids, which had been reduced to only three surviving lineages (Brayard et al., 2006, 2007; Brayard and Bucher, 2015; Dai et al., 2019), together with a few other groups, i.e., conodonts and foraminifers, recovered their diversity much faster than other organisms following the extinction event (Brayard et al., 2009; Song et al., 2011, 2013). Furthermore, recent discoveries have disclosed the existence of a remarkably complex and diversified marine ecosystem of earliest Spathian age, i.e., the Paris Biota, mainly from southeastern Idaho and to a lesser extent from northeastern Nevada (Brayard et al., 2017; Smith et al., 2021). This surprisingly diverse biota consists of at least seven phyla and 20 distinct metazoan orders, thus demonstrating that marine life recovered its overall pre-extinction diversity at least in a paleoequatorial setting only ~2 million years after the PT extinction event (Brayard et al., 2017; Smith et al., 2021). And, an even older, extremely complex marine ecosystem recently reported by Dai et al. (2023a), i.e., the late Dienerian Guiyang Biota from Guizhou Province, South China, pushes the recovery of marine life back until only about 1 million years after the PT extinction event.

Aside from the Paris Biota, evidence of this recovery in the ammonoid record in the western U.S. basin at least for the Induan is quite rare, with well-documented occurrences limited

to just two localities, i.e., the late Griesbachian site at Crittenden Springs (Fig. 1A, B), northeastern Nevada (Jenks et al., 2021) and the late middle, early late Dienerian Candelaria site (Fig. 1B) in southwestern Nevada (Ware et al., 2011). The ammonoid record for the late Griesbachian in low-paleolatitude eastern Panthalassa was virtually non-existent prior to the discovery at Crittenden Springs, and, similarly, there was no record of early Dienerian ammonoids in eastern Panthalassa prior to the present work, except for one problematic occurrence in Arctic Canada. This supposition is based only on the presence of the early Dienerian index conodont *Sweetospathodus kummeli* in an uppermost stratigraphic sample collected by Orchard (2008) from the upper Griesbachian *Bukkenites strigatus* Zone. Because of this discovery and the later realization that the ammonoid genus *Bukkenites* occurs in both the Griesbachian and Dienerian of the NIM (Dai et al., 2023b), the *B. strigatus* Zone is now considered as straddling the Griesbachian/Dienerian (G/D) boundary.

Ongoing reconnaissance in the Dinwoody Formation of the Thaynes Group at Crittenden Springs, following the earlier discovery of late Griesbachian ammonoids and nautiloids (see Jenks et al., 2021), has resulted in the discovery of additional significant ammonoid and nautiloid occurrences. These include an early Dienerian ammonoid and nautiloid fauna (Figs. 2A, 3), which includes gyronitids, as well as a second, late Griesbachian ammonoid site (L-13032, Figs. 2B, 3) that is stratigraphically higher than the original site (L-12682, Fig. 2B). Of notable significance, the gyronitid ammonoids represent the first documented occurrence of this genus outside the Tethys and South Primorye (Fig. 4). These cumulative ammonoid and nautiloid discoveries aptly demonstrate the “under-sampled” nature of the Dinwoody Formation, at least in the Crittenden Springs area, and they certainly provide motivation for a

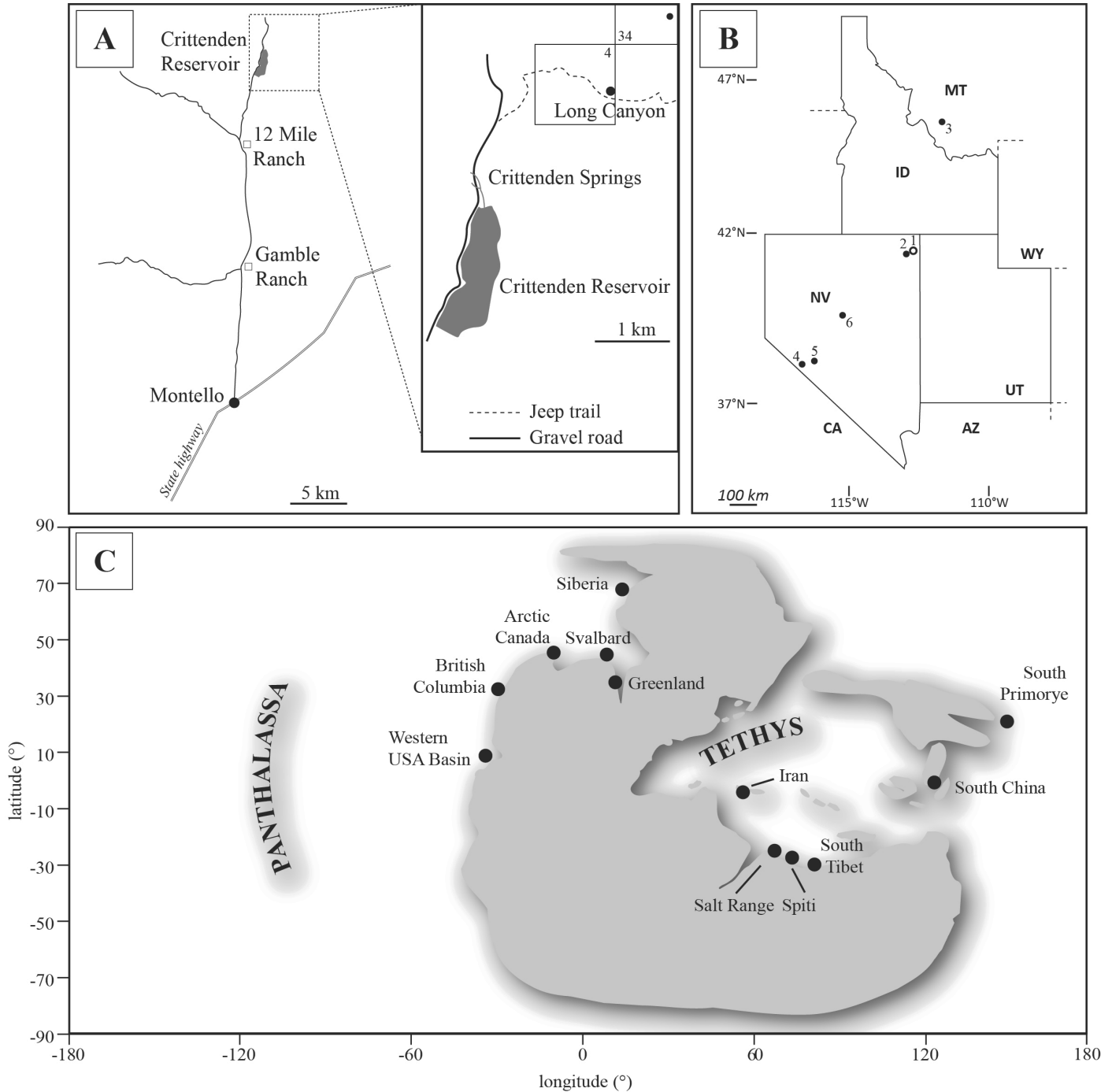


FIGURE 1. **A.** Generalized map showing location of early Dienerian ammonoid and nautiloid sites in the Crittenden Springs-north area indicated by upper black dot, which represents seven successive fossiliferous beds in the vicinity of the center of Sec 34, and the new late Griesbachian ammonoid site indicated by lower black dot in the SE1/4 of Sec 4 just north of the Long Canyon jeep trail (section boundaries not to scale). **B.** Location of Crittenden Springs area in relation to other western USA Dienerian and Griesbachian localities mentioned in text: 1) Crittenden Springs, 2) Immigrant Canyon, 3) Frying Pan Gulch, 4) Candelaria, 5) Willow Spring, 6) Marysville Canyon. **C.** Early Triassic paleoposition of the western USA basin in relation to other world-wide localities discussed in text. (A to C modified after Jenks and Brayard (2018) and Jenks et al. (2021).

closer examination of outcrops in other areas of the Dinwoody depositional basin.

Even though the present work is focused mainly on early Dienerian and to a lesser extent on late Griesbachian ammonoids found in the study area, co-occurring conodonts contribute significantly to our understanding of the correlation between ammonoid and conodont biostratigraphy. The conodont *Sweetospathodus kummeli* is generally regarded as a basal

Dienerian marker (Sweet, 1970; Paull, 1980; Mullen, 1985; Krystyn et al., 2003; Brosse et al., 2017; Han et al., 2022). However, reports of basal early Dienerian ammonoids and confirmed occurrences of *S. kummeli* in the same section are relatively rare (e.g., Sweet, 1970). Therefore, if *S. kummeli* is to become widely accepted as a marker for the Griesbachian/Dienerian Boundary (GDB), it is vitally important that its first occurrence (FO) be reported when found with co-occurring

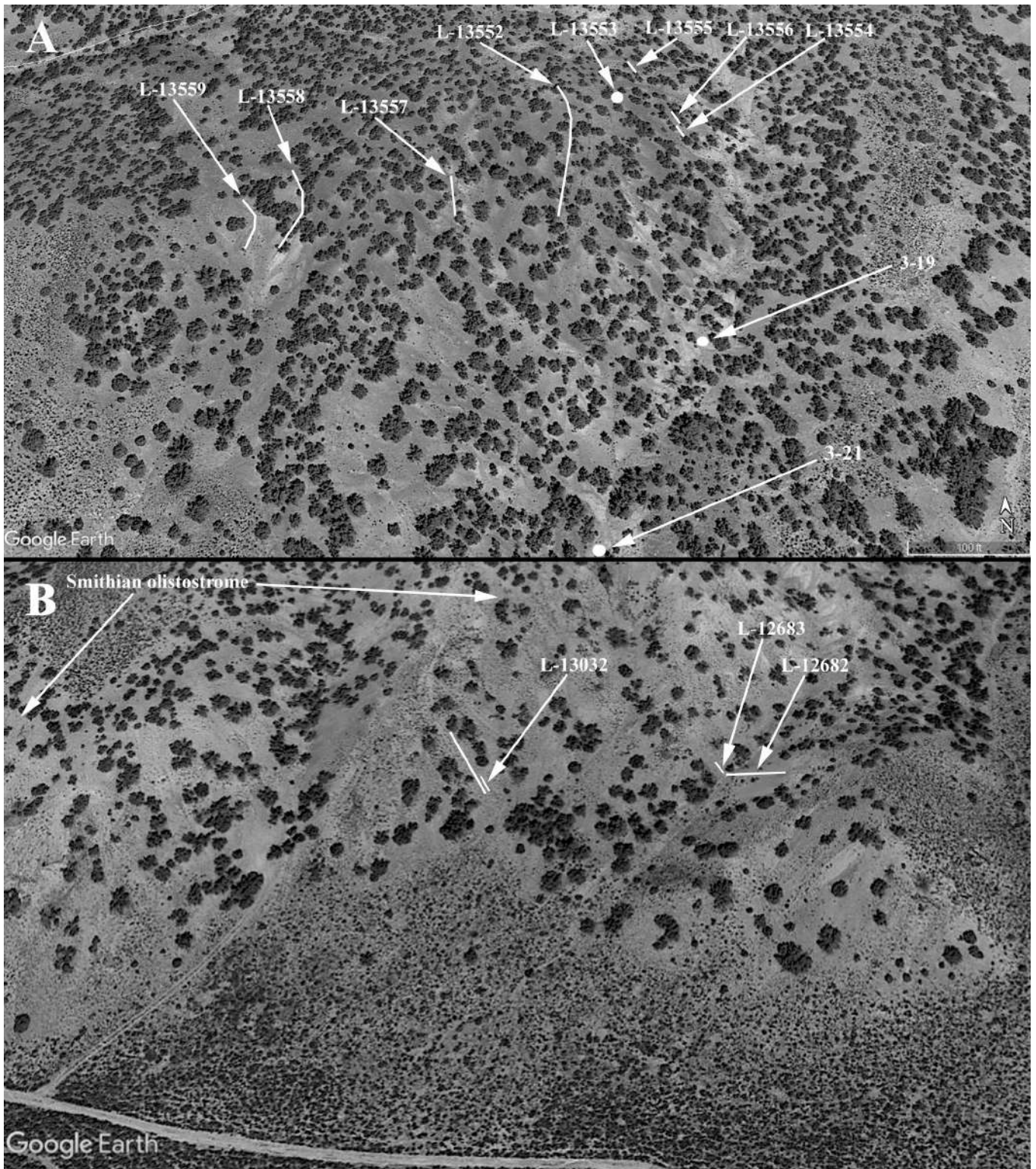


FIGURE 2. Google Earth images. **A**, early Dienerian ammonoid and nautiloid localities in the Dinwoody Formation in the Crittenden Springs-north area (Sec 34, T43N, R69E). **B**, location of new late Griesbachian ammonoid site (L-13032) in the Dinwoody Fm in relation to original site (L-12682, L-12683), whose ammonoids and nautiloids were described in NMMNH&S Bulletin 86. Solid white lines in (A) represent relevant outcropping beds (oldest to youngest in westerly direction) containing in, **L-13556**, *Gyronites rigidus* and *Ussuridiscus varaha*, **L-13554**, *Gyronites rigidus* and *Ussuridiscus varaha*, **L-13555**, *Gyronites rigidus*, *Ussuridiscus varaha* and *Ghazalaites roohiae*, **L-13552**, *Gyronites rigidus*, **L-13557**, *Gyronites frequens*, **L-13558**, *Gyronites frequens* and *Proptychites* sp., **L-13559**, *Gyronites frequens*, *Gyronites bullatus* and *Xiaohenautilus* n. sp. Float locality, **L-13553**, white circle, *Gyronites rigidus*, *Ussuridiscus varaha* and gen. et sp. indet. Float localities **3-19** and **3-21** represent hand-size float blocks found in “*Gyronites* gulley” (contained ammonoids not included in present work). Long solid white line in (B), represents a ~25 m thick section, in which float slabs of bivalve coquina containing *Wordieoceras wordiei* and *W. mullenae* specimens were found in a ~2 m wide x 7 m long band, **L-13032** (represented by the short white line, not to scale) on the lower hillside.

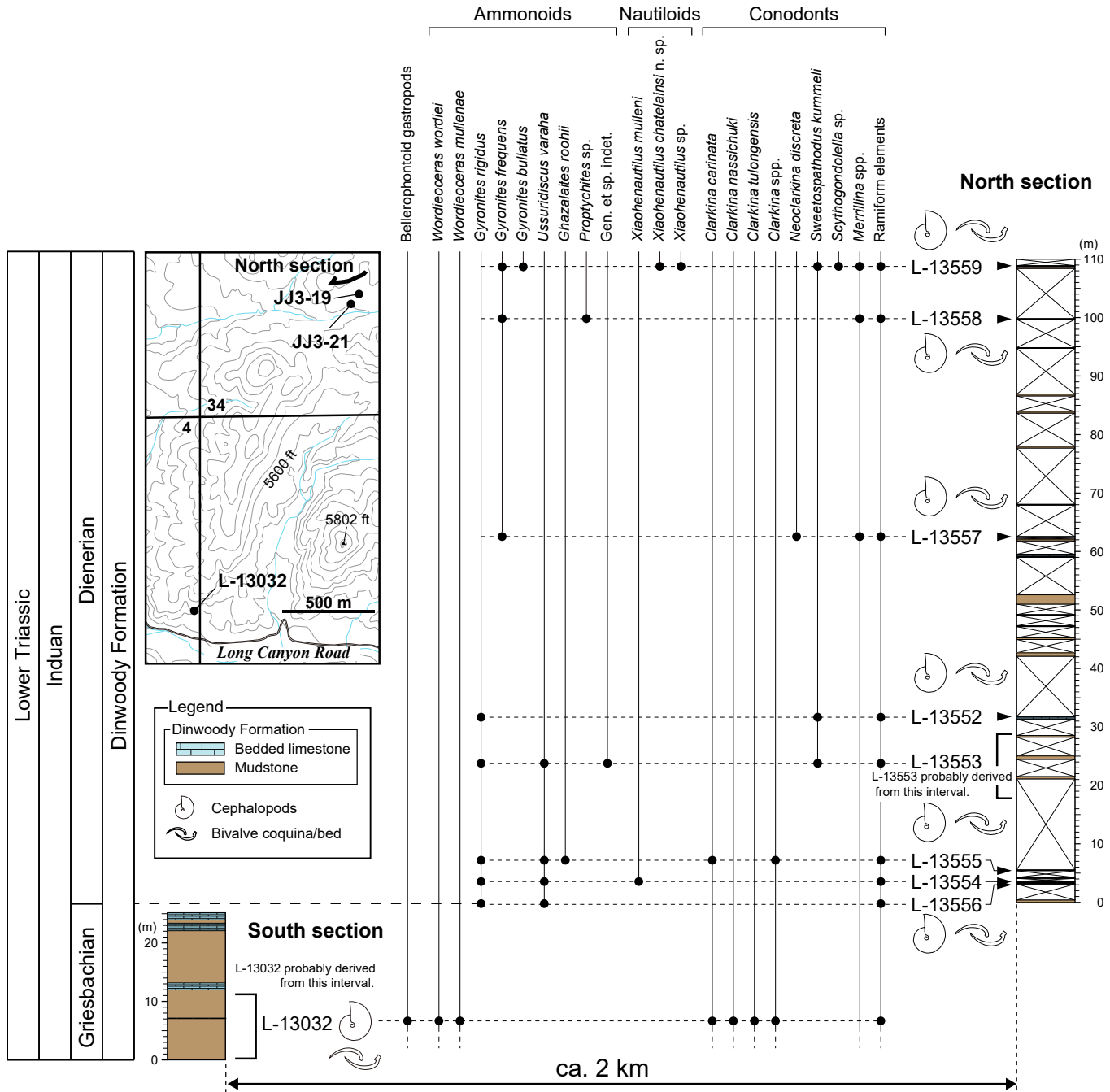


FIGURE 3. Columnar section showing stratigraphic occurrences of early Dienerian ammonoids, nautiloids, and conodonts in the Crittenden Springs-north area and the new late Griesbachian ammonoid locality (L-13032) at the southern end of the outcrop area.

basal Dienerian ammonoids. Our data from the study area clearly meets this requirement and contributes to the discussion of the GDB.

LOCALITY AND GEOLOGICAL CONTEXT

Location

The early Dienerian ammonoid and nautiloid site is located on U.S. public land (BLM) in the Crittenden Springs-north area (Sec 34, T43N, R69E) in the vicinity of a shallow, NE-SW trending drainage gully (informally termed *Gyronites* gully) about ~1.9 km north of Long Canyon (Figs. 1A, 2A), while the newly found Griesbachian ammonoid site is also located on BLM land in the SE1/4 Sec 4, T42N, R69E, on a gently sloping,

south-facing hill ~130 m north of the Long Canyon road and ~150 m east-northeast of the original classic Crittenden Springs Smithian ammonoid site (Figs. 1A, 2B) (Kummel and Steele, 1962; Jenks, 2007; Jenks et al., 2010; Jenks and Brayard, 2018; Maekawa and Jenks, 2021). This general area is located ~32 km north of Montello, Elko County, Nevada, and ~ 4 km and ~2.3 km, respectively, northeast of the abandoned ranch house at the north end of the Crittenden Reservoir (Fig. 1A).

Dinwoody Formation: History and Depositional Basin Setting, Lithostratigraphy and Depositional Basin Outcrops

Blackwelder (1918) named the Dinwoody Formation, the oldest Triassic unit of the Thaynes Group, for outcrops in Dinwoody Canyon in the Wind River Range of north-central

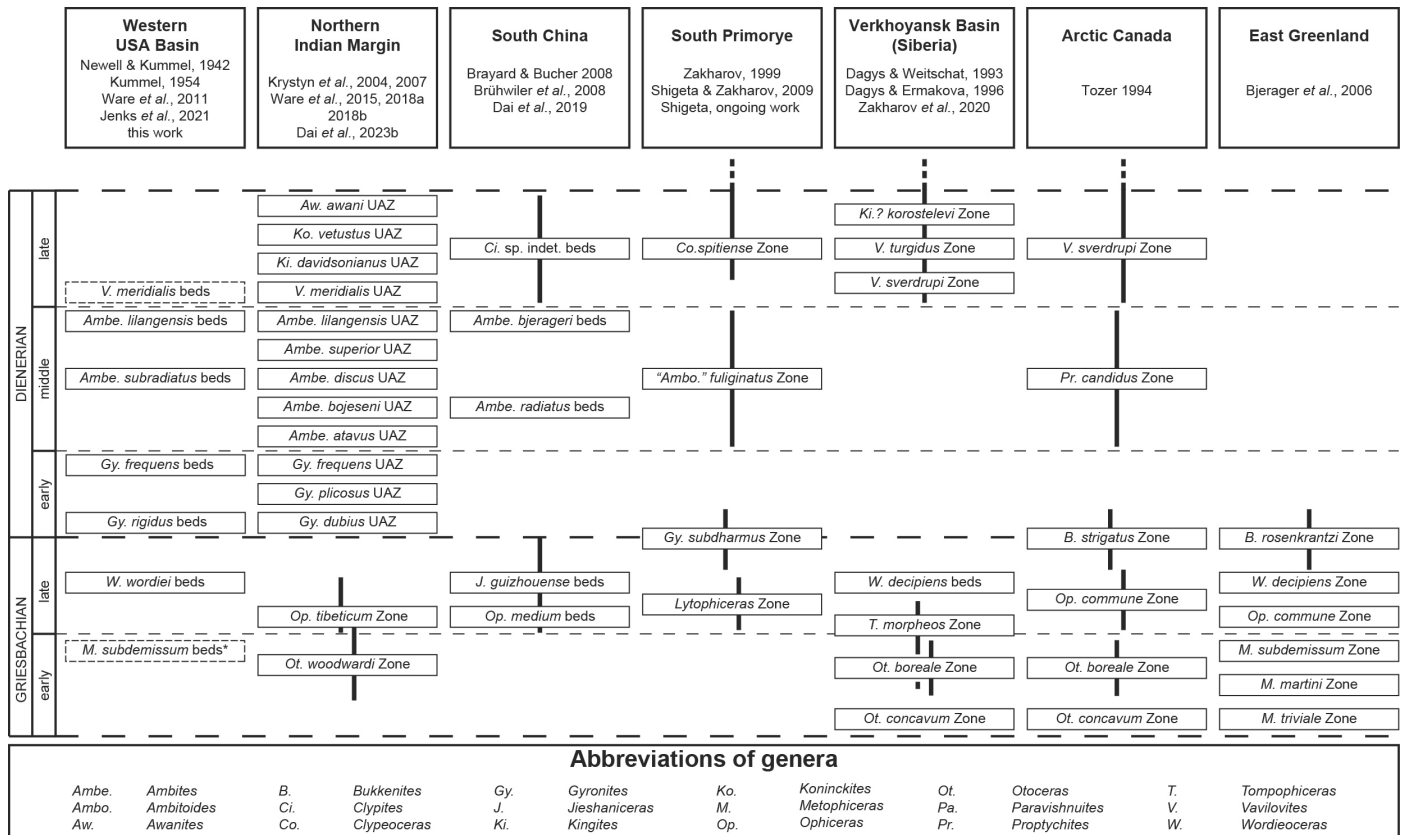


FIGURE 4. Induan ammonoid zonation of the western USA basin and correlation with other global occurrences. Bold black vertical bars represent uncertain correlation. Dashed line boxes encompassing *Vavilovites meridialis* beds and *Metopliceras subdemissum* beds of western USA basin represent uncertain stratigraphic occurrences within late Dienerian and early Griesbachian, respectively. Similarly, asterisk marking *M. subdemissum* beds denotes uncertain ammonoid identification. Note: Ongoing work by Ware is expected to significantly modify the zonation of Bjerager et al. (2006) for East Greenland. UAZ = Unitary Association Zone. Figure modified after Bjerager et al. (2006); Ware et al. (2018a); Jenks et al. (2021); Dai et al. (2023b).

Wyoming (Kummel, 1954; Paull, 1980). Resting unconformably on Permian rocks, the Dinwoody Formation is overlain either by basal rocks of the Thaynes Group or by red beds of the Woodside Formation in the more easterly areas (Paull, 1980). The Dinwoody sea, restricted to the northern part of an elongate epicontinental marine basin, i.e., the Sonoma foreland basin, by an east-trending structural high, extended to the northeast through northeastern Nevada, northwestern Utah, south-central and southeastern Idaho (Paull and Paull, 1994), and then northward along the Wyoming-Idaho border into southwestern Montana (Collinson and Hasenmuller, 1978; Wardlaw et al., 1979; Paull, 1980, Carr, 1981; Carr and Paull, 1983; Mullen, 1985; Caravaca et al., 2017; Jenks et al., 2021). According to Silberling (1973), the Sonoma orogenic belt probably formed the western shoreline of the Dinwoody Sea, but very little is known about this area because of the lack of outcrops.

Lithostratigraphic Divisions

Newell and Kummel (1942) initially divided the Dinwoody Formation in the type area in Wyoming into three lithostratigraphic units, i.e., the basal siltstone, the *Lingula* zone and the *Claraia* zone, but Kummel (1954) later determined that this classification was of little practical value in southeastern Idaho and other areas. Later, Hofmann et al. (2013) came to the same conclusion following their investigation of nine sections in southwestern Montana, southeastern Idaho and northern Utah. Paull (1980) stated that sediments across the depositional basin commonly consist of an interbedded complex of olive-gray to tan, calcareous silty shale, brown to gray limestone and olive-drab calcareous siltstone (Jenks et al., 2021). In the greater

central part of the basin, which includes the Crittenden Springs area, the formation consists of a lower shaly unit (deeper water facies) and an upper siltstone and limestone unit (Mullen, 1985a). In the immediate Crittenden Springs region (classical southern outcrop area and northern area of this study), Paull (1980) and Mullen (1985a), both of whom sampled outcrops for conodonts, roughly divided the Dinwoody Formation into two lithological units, i.e., a lower unit consisting mainly of poorly exposed olive-gray shales with a few thin inter-beds of olive-gray, silty limestone, and a generally more resistant upper unit comprised of inter-bedded thin, to massive-bedded gray limestone and thin to medium-bedded gray calcareous siltstone (Jenks et al., 2021).

Outcrops of the Dinwoody Formation occur in all states originally covered by the Dinwoody sea (see Figure 1B) and vary in thickness from ~30 m at the type locality (as redefined by Newell and Kummel, 1942) to ~740 m near the depo-center in southeastern Idaho (Paull, 1980; Jenks et al., 2021). In the more easterly areas, the formation is overlain by red beds of the Woodside Formation, whereas to the west, its uppermost limit is arbitrarily placed at the base of the *Meekoceras*-bearing lower limestone member (or equivalents) of the Thaynes Group (*sensu* Lucas et al., 2007; Paull, 1980; Jenks et al., 2021). Deposition was limited to the northern part of the basin because of the east-trending structural high bisecting the Sonoma foreland basin (Mullen, 1985a, b; Jenks et al., 2021), which apparently was located just a short distance to the south of the study area (Collinson and Hasenmuller, 1978; Wardlaw et al., 1979; Paull, 1980; Carr and Paull, 1983; Mullen, 1985a, b; Caravaca et al., 2017; Jenks et al., 2021). See Jenks et al. (2021) for a more detailed discussion of the history, lithostratigraphy and

depositional basin outcrops of the Dinwoody Formation.

Study Area Outcrops

Exposures of marine Lower Triassic strata crop out just north of the Long Canyon Road in the vicinity of the classical Smithian ammonoid collecting area and extend in a northeasterly direction for ~8 km, covering an area of ~33 km² (Clark, 1957; Mullen, 1985a; Jenks and Brayard, 2018; Jenks et al., 2021). Hope and Coats (1976, U.S.G.S. Open-file Map 76-779) mapped the area as part of their larger Geology of Elko County, Nevada project but didn't differentiate the various Lower Triassic outcrops. Mullen (1985a) mapped the entire area as part of her conodont studies and differentiated the following units, in ascending order: Permian undifferentiated and Thaynes Group (Dinwoody Formation, *Meekoceras* limestone, black limestone, calcareous siltstone and limestone, and *Pentacrinus* limestone). According to Mullen (1985a), the Dinwoody Formation was found to be in normal stratigraphic sequence with underlying Permian rocks at only one location, which was chosen as the base of her measured section. This particular area is located on Winecup-Gamble Ranch land and was inaccessible to our study. Elsewhere in the area, the Permian-Dinwoody Formation contact is either covered, or Permian outcrops are in fault contact with the Dinwoody Formation (Mullen, 1985a).

Our field work over a period of several years has led to a different stratigraphic interpretation of the lower part of the "Thaynes Formation" in the southern portion of the study area. The aforementioned typical *Meekoceras*-bearing, massive limestone member present in most outcrop areas, i.e., SE Idaho, Confusion Range, Utah, Palomino Ridge, Nevada, etc. (Kummel, 1954; Hose and Repenning, 1959; Jattiot et al., 2017), is missing, and, instead, the Dinwoody Formation is overlain by an apparent debris-flow deposit or olistostrome of uncertain thickness (estimated to be 8-10 m) consisting of unconsolidated sediments and various dissimilar exotic blocks or olistoliths (Fig. 5), i.e., siltstone debris, unfossiliferous limestone boulders of varying sizes, crinoid-bearing blocks and numerous but discontinuous, ~1 m thick Smithian ammonoid-bearing blocks, most of which are overturned (Jenks, 2007; Jenks et al., 2010; Jenks and Brayard, 2018; Maekawa and Jenks, 2021; Maekawa and Jenks, in press). That this chaotic occurrence of dissimilar rocks was caused by a submarine debris flow or slump is compellingly suggested by the appearance of the unconsolidated sediments and the inverted occurrence of Smithian ammonoid faunas in the ammonoid-bearing blocks (Maekawa and Jenks, in press). Furthermore, it is suggested that the supposedly Spathian-aged "black limestone" of Clark (1957) and Mullen (1985a), together with the "dark gray calcareous mudstone" of Maekawa and Jenks (in press), actually encompasses this olistostrome (Maekawa and Jenks, in press). This hypothesis is additionally supported by the presence of numerous "slump structures" in the black limestone that were pointed out to JFJ and KGB (H. Bucher, personal commun. 2014) and later recognized independently by TM.

Although this interpretation has been gradually formulated over the past several years (Maekawa and Jenks, 2021, in press), the unusual nature of this interval occupying the lower part of the "Thaynes Formation" first became apparent in 1988 when part of the classic site was bulldozed to expose additional ammonoid-bearing blocks for a study of ammonoid color patterns by R.H. Mapes (Mapes and Sneek, 1987; Mapes and Davis, 1996; Gardner, 2000; Gardner and Mapes, 2000).

Descriptions of Newly Found Early Dienerian and Late Griesbachian Ammonoid Sites

Early Dienerian Ammonoid and Nautiloid Site

Specimens of the early Dienerian ammonoid genus *Gyronites* were first found in 2019 in a few hand-size, float

pieces of bivalve coquina scattered along a ~95 m long section of "Gyronites gulley", i.e., JJ3-19 and JJ3-21 in the Crittenden Springs-north area (Fig. 2A). Then, between late 2022 and late 2023, seven successive beds of fossiliferous limestone or bivalve coquina containing rare *Gyronites* specimens were discovered, i.e., *Gyronites rigidus* in NMMNH L-13556, L-13554, L-13555 and L-13552, *Gy. frequens* in L-13557, L-13558 and L-13559, and *Gy. bullatus* in L-13559, in ascending order, in a ~110 m thick sequence in the gently sloping hills on the north side of the gulley (Figs. 2A, 3). Beds L-13556, L-13554 and L-13555 also yielded very rare specimens of *Ussuridiscus varaha* and *Ghazalaites roohii*. A hand-size float block, i.e., L-13553, found above L-13555 and below L-13552 also contained a specimen of *Ussuridiscus varaha* together with a very small specimen classified as gen et sp. indet. Topographic constraints limited this float block's origin to just above L-13555 but not from L-13552 or higher. Bed L-13558 also yielded one specimen of *Proptychites* sp. Outcrops of the relatively thin lower beds, i.e., L-13556, L-13554 and L-13555, are each only ~1 to 2 m in length and occur within a narrow stratigraphic interval (~1-1/2 m) over a very limited area, i.e., ~40 meters along strike; exposures are very obscure, and nowhere are they exposed in succession. Abundant trees, sagebrush and intermittent soil cover make it nearly impossible to trace these beds along strike. In contrast, the upper beds, i.e., L-13552, L-13557, L-13558 and L-13559 are significantly thicker and outcrops are easily traceable for several meters along strike, especially beds L-13552, L-13558 and L-13559. Most beds crop out with a similar attitude; that is, they mainly strike from NW to N-NW and dip rather steeply to the SW. However, the exposures of beds L-13552, L-13558 and L-13559 are of such length that their outcrops follow the contour of the relatively small hills as seen in Figure 2A. Many, if not all of the above beds probably crop out in "Gyronites gulley" to the south, but it is impossible to trace them back because of the distance involved and intervening soil cover.

A badly weathered nautiloid, *Xiaohenautilus mulleni*, was found as float more or less along strike about 2 m to the east of L-13554. Additionally, bed L-13559 yielded two, fairly well-preserved but incomplete nautiloid specimens, which represent a new species of *Xiaohenautilus*, i.e., *X. chatelaini* n. sp.

Preservation of the *in situ* ammonoid specimens in the bivalve coquina beds ranges from mostly poor to good and is largely dependent upon the degree to which the co-occurring bivalves are fragmented. For example, bed L-13552 is mainly composed of highly fragmented shell debris, which is indicative of a high-energy depositional environment, and consequently, many ammonoid specimens are fragmented and distorted. Bed L-13554 mainly consists of a hard, silty limestone with minor amounts of coquina, and preservation is generally poor, with most specimens only partially preserved (ghost preservation) and badly distorted. Conversely, beds L-13555 and L-13556 consist of relatively clean, fairly well-preserved bivalve coquinas, and ammonoid preservation is usually much better. Suture lines are not always preserved, but the morphological features of the specimens leave little doubt as to their identity. Likewise, the two specimens representing the new nautiloid taxon from bed L-13559, which is composed mainly of the same well-preserved bivalve coquina, are surprisingly well-preserved, though incomplete.

New Late Griesbachian Ammonoid Site

The newly discovered late Griesbachian ammonoid site, i.e., L-13032, consisting of numerous 4-5 cm thick float slabs of a fairly well-preserved, ammonoid-containing bivalve coquina, is located on a gently sloping (~26°), south-facing hillside about 85 m west of the original site (Fig. 2B)(Jenks et al., 2021: L-12682). This ~25 m thick section (Fig. 3), which lies within a faulted block that appears not to be in the same stratigraphical sequence

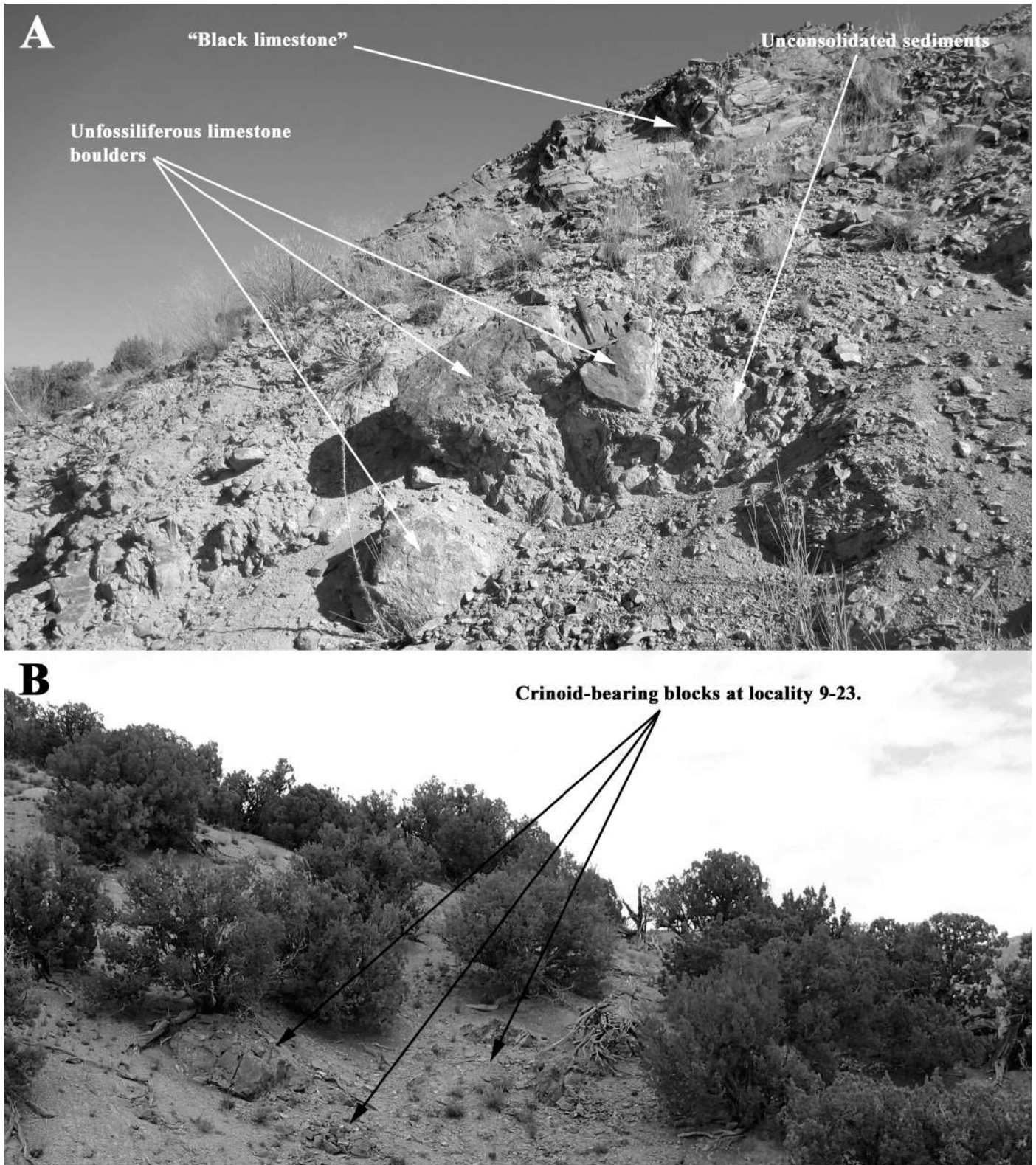


FIGURE 5. Smithian olistostrome. **A.** Debris-flow deposit at classic Smithian ammonoid collecting area at southern end of outcrop consisting of unconsolidated sediments (shales, siltstone fragments) and large unfossiliferous boulders. Overturned 1 m thick ammonoid-bearing block (5-76, in Jenks and Brayard, 2018) was located just below and to left of photo, but further excavation is prohibited by excessive overburden. It is hypothesized that “black limestone” at top of photo is actually the olistostrome binder. **B.** Crinoid-bearing blocks (olistoliths) located ~140 m northeast of photo in A. (modified after Maekawa and Jenks, in press).

as the original section, consists mainly of poorly exposed shales and two ~1 m thick successions of limestone beds that dip at about 45° to the north-northwest. Valley fill covers the lower part of the section, and bulldozer scree obscures the contact with the overlying Smithian olistostrome. Due to poor exposures and concealed faulting, it's not yet exactly certain how the exposed part of this faulted section is related stratigraphically to the section at L-12682 and L-12683, but the bivalve coquina float slabs almost certainly originated stratigraphically higher than the original *in situ* fauna. These float slabs, designated as L-13032, have been found only within a narrow, ~2 m wide down-slope band that extends over the lower ~7 m of the hillside, and trenching efforts through the entire ~25 m thick succession have failed to pinpoint their source. This failure combined with the absence of float slabs along strike on either side of this narrow band leads us to suspect that their source consisted of a lense or bivalve mound rather than a continuous bed.

Preservation of the *Wordieoceras wordiei* specimens found in these float slabs ranges from poor to quite good. Shell material is not preserved, but some specimens exhibit well-preserved suture lines, and in contrast with the original late Griesbachian site, many specimens include nearly complete, undistorted body chambers.

DIENERIAN AMMONOID BIOSTRATIGRAPHY NORTH AMERICA

Western USA Basin

Dienerian ammonoids in the western USA basin are extremely rare. Indeed, the ammonoids of this study represent not only the first confirmed report of early Dienerian ammonoids in the region, but in North America as well, aside from the aforementioned probable extension of the upper Griesbachian *Bukkenites strigatus* Zone into the lower Dienerian in Arctic Canada (Orchard, 2008). The studied fauna correlates broadly with the entire early Dienerian of the NIM, which consists of a three-fold subdivision, i.e., the *Gyronites dubius*, *Gy. plicosus* and *Gy. frequens* Unitary Association Zones (UAZ), in ascending order as defined by Dai et al. (2023)(Fig. 4). Although *Gy. dubius*, the eponymous taxon of the lowest UAZ, has not been found in the study area, the lower beds (L-13556, L-13554, L-13555 and L-13552) do contain three taxa that are common components, i.e., *Gy. rigidus*, *U. varaha* and *Ghazalaites roohiae*. The higher beds (L-13557, L-13558 and L-13559) contain *Gy. frequens*, the eponymous taxon of the uppermost UAZ, as well as two other common taxa, i.e., *Gy. bullatus* and *Proptychites* sp. (Fig. 4). Ammonoids representative of the middle UAZ have not been found in the study area even though sufficient space exists in the ~30 m thick interval between the highest *Gy. rigidus* and lowest *Gy. frequens* occurrences. However, this interval mainly consists of poorly exposed shales without significant outcrops.

The only other well documented Dienerian ammonoid fauna in the western USA basin is the late middle and early late Dienerian fauna reported by Ware et al. (2011) from the Candelaria Formation near the old mining camp of the same name (Fig. 1B) in Mineral and Esmeralda counties, Nevada (Muller and Ferguson, 1939; Jenks et al., 2021). Ware et al. (2011) originally considered these faunas, i.e., the *Ambites lilangensis* assemblage, as well as two informal ammonoid horizons, to be of early Dienerian age, but the subsequent taxonomic revision of Dienerian ammonoids from the NIM by Ware et al. (2018a, b) has demonstrated that the Candelaria fauna is late middle to early late Dienerian in age (Jenks et al., 2021).

Poole and Wardlaw (1978) discussed an additional outcrop of the Candelaria Formation located near Willow Spring in the southern Toquima Range, Nye County, Nevada (Fig. 1B), about 80 km northeast of the Candelaria locality (Jenks et al., 2021). Poorly preserved ammonoids contained in a 3 to 12 m thick

limestone bed are assumed to represent the same taxa as at the Candelaria locality (Poole and Wardlaw, 1978), but the fauna has not been studied due to its extremely poor preservation (Jenks et al., 2021). Poole and Wardlaw (1978) also mentioned the occurrence of an ammonoid fauna in Marysville Canyon on the west side of the Toiyabe Range in northern Nye County, identified as of probable late Griesbachian age (Fig. 1B), similar to the fauna in the lowermost beds of the Candelaria Formation at Willow Spring (Jenks et al., 2021). Again, this fauna has not been studied due to its presumed poor preservation. And, lastly, Kummel (1954) referred to two poorly preserved “Gyronitan” ammonoid faunas found in succession in the Dinwoody Formation at Frying Pan Gulch (Fig. 1B), northwest of Dillon, Beaverhead County, Montana (Jenks et al., 2021). These were identified as *Prionolobus* and *Koninckites* in the lower horizon and *Kymatites*, *Koninckites* and *Xenodiscoides* in the upper horizon (Kummel, 1954), but Kummel neither illustrated the specimens nor provided precise collection localities (Jenks et al., 2021). Given their poor preservation and the extensive revision of Dienerian ammonoid taxa in recent years, it is difficult to ascertain the exact age of these faunas, but it is assumed they are either early or middle Dienerian (Jenks et al., 2021).

These four localities essentially represent all that is known regarding Dienerian ammonoids within the western USA basin.

British Columbia, Canada

Tozer (1984, 1994) documented two Dienerian ammonoid zones in the Toad Formation of northeastern British Columbia, i.e., the *Proptychites candidus* Zone of middle Dienerian age and the late Dienerian *Vavilovites sverdrupi* Zone (Dai et al., 2023b). The latter is subdivided into three subzones, i.e., the *Koninckites dimidiatus*, *Vavilovites obtusus*, and *Kingites discoidalis* Subzones, in ascending order (Tozer, 1984, 1994). Following an examination of Tozer's collection at the Geological Survey of Canada, DW in Dai et al. (2023b), concluded that many of the Dienerian taxa from British Columbia are not conspecific with “corresponding taxa” in Arctic Canada. In particular, specimens from the Toad Formation, identified by Tozer (1984, 1994) as *Proptychites candidus* and *Vavilovites sverdrupi*, are not the same as the taxa from the Arctic, and are actually closer to taxa from the Southern Neotethys (Dai et al., 2023b).

Arctic Canada

The Dienerian is limited to two zones in Arctic Canada, i.e., the middle Dienerian *Proptychites candidus* Zone and the late Dienerian *Vavilovites sverdrupi* Zone; both eponymous ammonoids occur on the south side of Diener Creek, Ellesmere Island, the type locality of the Dienerian Stage (Tozer, 1965). Prior to Orchard's (2008) conodont work in the Arctic Islands, there had been no record of early Dienerian ammonoids in this region. But, the discovery of the early Dienerian conodont, i.e., *Sweetospathodus kummeli*, in the uppermost stratigraphic level of the late Griesbachian *Bukkenites strigatus* Zone indicates that this zone may extend up into the Dienerian (Orchard, 2008; Ware et al., 2018a; Dai et al., 2023).

BOREAL REALM

Greenland

Dienerian-age sediments are unknown in Greenland. However, as in Arctic Canada, the more or less equivalent late Griesbachian *Bukkenites rosenkrantzi* Zone may extend up into the Dienerian (Fig. 4) (Ware et al., 2018a; Dai et al., 2023b).

Svalbard

Weitschat and Dagys (1989) and Dagys and Weitschat (1993) documented the presence of the late Dienerian *Vavilovites sverdrupi* Zone (Fig. 4). Early and middle Dienerian ammonoids have not yet been reported from Svalbard (Dai et al., 2023b).

Siberia

There is no record of early and middle Dienerian ammonoids in Siberia, but Dagys and Ermakova (1996) recorded three late Dienerian ammonoid zones from the eastern Verkhoyansk region of northeastern Siberia, i.e., the *Vavilovites sverdrupi* Zone, *V. turgidus* Zone and *Kingites? korostelevi* Zone, in ascending order (Fig. 4). The *V. turgidus* Zone is subdivided into two subzones, i.e. the *V. subtriangularis* Subzone and the *V. umbonatus* Subzone (Dagys and Ermakova, 1996). Although the *V. sverdrupi* Zone is readily correlatable with other Boreal regions, the *V. turgidus* and *K? korostelevi* Zones consist only of endemic taxa and cannot be accurately correlated with other areas (Dai et al., 2023b).

NORTHERN INDIAN MARGIN

Salt Range, Pakistan

The NIM has been long known for its comprehensive Early Triassic ammonoid record. Indeed, ammonoids discovered in the Salt Range by Andrew Fleming in the mid-19th century, and later described by de Koninck (1863), are now recognized as comprising the very first Dienerian-age ammonoid fauna ever described, and Waagen (1895) is also well known for his very thorough study of Early Triassic ammonoids from the Salt Range (Ware et al., 2018a). Relatively little work was centered on Dienerian ammonoids in this region from the time of Waagen until Guex (1978) described a relatively small but well-documented Dienerian, Smithian and Spathian ammonoid assemblage, and suggested an alternative three stage subdivision of the Early Triassic (Jenks et al., 2015; Ware et al., 2018a). Consequently, Dienerian ammonoids remained poorly known and in need of extensive revision for the next 100+ year period (Jenks et al., 2015). Then, beginning in 2007, researchers from the University of Zurich's Paleontological Institute and Museum initiated a multi-year, carefully controlled bedrock sampling program in several areas in the Salt Range, i.e., Nammal, Chidru, Amb and Wargal, which eventually led to a thorough taxonomic revision of Dienerian ammonoids (Ware et al., 2018a). This revision facilitated the development of a biostratigraphic scheme consisting of 12 successive regional ammonoid zones (Fig. 4), which represents by far the most complete record of Dienerian ammonoids in the world (Ware et al., 2018a).

According to Ware et al. (2018a), the Early Dienerian ammonoid record in the Salt Range, notwithstanding the potential presence of hiatuses and condensed deposits, also exhibits the most expanded and diverse faunal succession known anywhere in the world. Ammonoid zonation in the lower Dienerian, which is based on the genus *Gyronites*, includes three regional zones, i.e., the *Gy. dubius*, *Gy. plicosus* and *Gy. frequens* zones, in ascending order (Ware et al., 2018a).

Middle Dienerian ammonoid zonation, based on the genus *Ambites*, includes five regional zones, i.e., the *A. atavus*, *A. radiatus*, *A. discus*, *A. superior* and *A. lilangensis* zones, in ascending order (Ware et al., 2018a).

And, lastly, ammonoid zonation for the upper Dienerian consists of four regional zones, i.e., the *Vavilovites* cf. *V. sverdrupi*, *Kingites davidsonianus*, *Koninckites vetustus* and *Awanites awani* zones, in ascending order (Ware et al., 2018a).

Spiti, Hamachal Pradesh, India

Much like the Salt Range of Pakistan, the Spiti region is also well known for its all-inclusive record of Lower Triassic ammonoids (Ware et al., 2018b). The region's history of ammonoid study dates back to late 19th and early 20th centuries, when ammonoid study pioneers, i.e., Diener (1897) and Krafft and Diener (1909), published comprehensive monographs dealing with Lower Triassic ammonoids (Ware et al., 2018b). And, as with the Salt Range, field work focusing on Lower Triassic ammonoids ceased for many decades, i.e., about 80 years, until

the mid-1990's, when Leopold Krystyn began work that was aimed more at establishing a proposal for a GSSP candidate for the Induan/Olenekian boundary (Dienerian/Smithian) rather than on Triassic ammonoid taxonomy and biostratigraphy (Krystyn et al., 2004, 2007a, b; Ware et al., 2018b). Then, researchers from the Paleontological Institute and Museum (University of Zurich) spent two field seasons (2008, 2009) conducting a carefully controlled bedrock sampling program in three areas, i.e., Mud, Guling and Lalung, that resulted in the discovery of characteristic Smithian ammonoids (Brühwiler et al., 2010) below the boundary proposed by Krystyn et al. (2007a, b). This field work eventually culminated in the revision and description of middle and late Smithian ammonoids by Brühwiler et al. (2012) as well as the revision of Dienerian ammonoids by Ware et al. (2018b).

Ware et al. (2018b) determined that the ammonoid biozonation in the Spiti region is very similar to that of the Salt Range, with the same three-fold subdivision, i.e., early, middle and late, comprising the Dienerian, and somewhat surprisingly, 10 of the 12 regional ammonoid zones documented for the Salt Range are present in Spiti (Fig. 4), with the same association of characteristic taxa in each zone (Ware et al., 2018b). The two Salt Range zones not recognized in the Spiti region include the middle Dienerian *Ambites superior* and the late Dienerian *Awanites awani* regional zones (Ware et al., 2018b).

South Tibet

In contrast with the Salt Range and Spiti regions, the Lower Triassic ammonoid record of South Tibet has only recently come to light, nearly 100 years after the pioneering work of Griesbach (1880), Waagen (1895), Diener (1897) and Krafft and Diener (1909) in the two classic areas (Dai et al., 2023b). Wang and He (1976) documented five Lower Triassic ammonoid zones in South Tibet, i.e., the Griesbachian *Otoceras latilobatum* and *Ophiceras sakuntala* Zones, the Dienerian *Gyronites psilogyrus* Zone, the Smithian *Owenites* Zone and the late Smithian to Spathian *Procarinites-Anasibirites* Zone (Dai et al., 2023b). After extensive bed by bed sampling in the Tulong section, Brühwiler et al. (2010) produced a high-resolution middle to late Smithian biostratigraphical scale based on six ammonoid beds (Dai et al., 2023b). Later, Zhang et al. (2017) described a small number of Griesbachian and Dienerian ammonoids from the Qubu section and documented three zones, i.e., the Griesbachian *Otoceras woodwardi* and *Ophiceras tibeticum* Zones and the middle Dienerian *Ambites* Zone (Dai et al., 2023b).

And, finally, following a very comprehensive, bed-by-bed ammonoid sampling program in four sections, i.e., Selong, Paizi, Qubu and Xialong, and an extensive statistical analysis, Dai et al. (2023b) documented a total of 23 ammonoid Unitary Association Zones, of which 10 zones represent the Dienerian (Dai et al. 2023b). Remarkably, these 10 zones are either identical or very similar to those of the Salt Range and Spiti regions, with the same two zones not recognized, i.e., the *Ambites superior* and *A. awani* zones (Dai et al., 2023b).

SOUTH CHINA

Reports of Induan ammonoids are relatively rare in South China, with only two ammonoid zones documented for the Griesbachian and three for the Dienerian (Fig. 4)(Dai et al., 2023b). Thus far, there is no record of early Dienerian ammonoid occurrences, but the middle Dienerian includes two zones, i.e., the *Ambites radiatus* and *Ambites bjerageri* Zones, and the late Dienerian includes one monospecific level, i.e., the *Clypites* sp. indet. beds (Brayard and Bucher, 2008; Dai et al., 2023b). Brühwiler et al. (2008) reported well-preserved Dienerian (and Griesbachian) ammonoids from the Luolou and Daye formations in northwestern Guangxi and southern Guizhou provinces, of which the Dienerian faunas constitute

the *A. radiatus* and *A. bjerageri* Zones. Later, Dai et al. (2019) documented well-preserved Dienerian (and Griesbachian) ammonoids representative of the same two zones from a large exposure (Gujiao section) created by new highway construction ~20 km southeast of Guiyang, the capital of Guizhou Province (Jenks et al., 2021). And, finally, Brayard and Bucher (2008) recognized the late Dienerian *Clypites* sp. indet. beds in one particular section of the Luolou Formation in northwestern Guangxi Province.

SOUTH PRIMORYE

Shigeta and Zakharov (2009) reported a sequence of abundant and well-preserved Griesbachian, Dienerian and early to middle Smithian ammonoid faunas from the Lazurnaya Bay and Zhitkov formations at Abrek Bay, South Primorye (Fig. 4). The topmost zone of the Griesbachian includes the controversial *Gyronites subdharmus* Zone, and the Dienerian portion of the succession consists of, in ascending order, the *Ambitoides fulginatus* Zone and the *Clypeoceras spitiense* Zone (Shigeta and Zakharov, 2009; see also Jenks et al., 2021).

Considerable controversy surrounds this zonation, in particular the placement of the *Gy. subdharmus* Zone in the Griesbachian (Jenks et al. 2021). Indeed, Ware et al., (2015, 2018b) and Dai et al., (2019; 2023b) disagree and place the *Gy. subdharmus* Zone in the early Dienerian. Nevertheless, the *Gy. subdharmus* Zone contains ammonoid co-occurrences not seen before in other regions that lend support to this designation (Jenks et al., 2021). This evidence speaks to the possibility that the *Gy. subdharmus* Zone may at least straddle the Griesbachian/Dienerian boundary (Fig. 4). Furthermore, according to Ware (personal comm., 3-31-2023), the G/D boundary is unclear elsewhere if based solely on ammonoids; that is, the boundary interval contains a mix of typical Griesbachian ophiceratids and Dienerian gyronitids. Continuing work by Shigeta et al. is expected to help settle this controversy.

IRAN

Korn et al. (2021) discussed the high-resolution stratigraphy of the Baghuk Mountain section in central Iran, which exhibits uninterrupted sedimentation across the Permian/Triassic boundary. They documented numerous fossiliferous levels containing ammonoids and conodonts within the Permian and Early Triassic portions of the section that also include two, closely spaced horizons, each of which contains a fairly well-preserved monospecific, early Dienerian ammonoid assemblage, i.e., *Gyronites* cf. *dubius* and *Ussuridiscus varaha*, in ascending order (Korn et al., 2021).

THE BASAL DIENERIAN INDEX CONODONT *SWEETSPATHODUS KUMMELI* AND THE GRIESBACHIAN/DIENERIAN BOUNDARY (GDB)

The present study has yielded abundant conodont elements belonging to 5 genera and 8 species from the early Dienerian ammonoid localities in the Crittenden Springs-north section (Fig. 1A) and the newly discovered late Griesbachian ammonoid site (L-13032) at the southern end of the outcrop area (Fig. 1A). From L-13032, we collected Griesbachian-age *Clarkina carinata*, *C. nassichuki*, *C. tulongensis* and *Clarkina* spp., and the Crittenden Springs-north section yielded a mixed Griesbachian/Dienerian-age fauna, i.e., *Sweetospathodus kummeli*, *Clarkina* spp., *Neoclarkina discreta*, *Scythogondolella* sp. and *Merrillina* spp. (Figs. 3, 17).

Jenks et al. (2021, fig. 5) reported late Griesbachian conodont assemblages from a section in the southern end of the outcrop area, i.e., levels 201507a and 201507b, located ~100 m northeast of the new late Griesbachian locality L-13032. Locality L-13032 most likely can be correlated with the stratigraphic interval between levels 201507b and a bed designated as 6 in Jenks et

al. (2021, fig. 5). These localities contain typical Griesbachian conodonts, i.e., *Clarkina carinata*, *C. taylorae*, *C. tulongensis* and *Hindeodus* spp., and the ammonoid and conodont data from L-13032 support this correlation.

Conodont workers have generally regarded the FO of *Sweetospathodus kummeli* to be indicative of the basal Dienerian (Sweet, 1970; Paull, 1980; Mullen, 1985a; Krystyn et al., 2003; Brosse et al., 2017; Han et al., 2022). However, in the present study, the FO of *Sweetospathodus kummeli* occurs in bed L-13552, which is about 30 m above the FO of the ammonoid *Gyronites rigidus* (L-13556), a component of the basal Dienerian *Gy. dubius* UAZ of the NIM (Ware et al., 2018a, b; Dai et al., 2023b). Han et al. (2022) reported a Griesbachian and Dienerian conodont assemblage containing *S. kummeli* from the Zaluch locality in the Salt Range and Narmia locality in the Surghar Range, Pakistan. According to these workers, the FO of *S. kummeli* at the Zaluch and Narmia localities occurs in the upper part of the Limestone Unit of the Kathwai Member of the Mianwali Formation. Ware et al. (2018a) reported the basal Dienerian ammonoids, i.e., *Gyronites dubius*, *Gy. rigidus*, *Bukkenites sakesarensis*, *Ghazalaites roohiae*, *Kyoktites* cf. *hebeiseni* and *Ussuridiscus varaha*, from the base of the Lower Ceratite Limestone of the Mittwali Member, Mianwali Formation, which crops out in the Nammal, Chidru, Amb and Wargal areas of the Salt Range. The Lower Ceratite Limestone occurs just above the Limestone Unit of the Kathwai Member. Thus, based on a summary of the work of Han et al. (2022) and Ware et al. (2018a), the FO of *S. kummeli* is slightly lower than the basal Dienerian ammonoids. Orchard (2008) reported a similar result from the Confederation Point Member at Griesbach Creek, Axel Heiberg Island, in the Canadian Arctic. According to Orchard (2008), *Neospathodus cristagalli* and *N. dieneri* occur at locality 51663, and *S. kummeli* is found at locality 51664, but the late Griesbachian ammonoid *Bukkenites strigatus* also occurs at locality 51664. Consequently, the *Bukkenites strigatus* Zone is now considered as straddling the Griesbachian/Dienerian (G/D) boundary (Orchard, 2008; Ware et al., 2018a; Dai et al., 2023b). Thus, the validity of the FO of *S. kummeli* as a marker for the G/D boundary in the Canadian Arctic is questionable. Data from our study area provide a result that differs from the FOs of the basal Dienerian ammonoids and *S. kummeli* from the NIM and Canadian Arctic. Thus, for the present study, it is much more accurate to determine the G/D boundary based on the FO of ammonoids, i.e., *Gyronites dubius*, *Gy. rigidus*, *Ghazalaites roohiae* and *Ussuridiscus varaha* rather than on the FO of the index conodont *S. kummeli*. Many more data are required in order to base the G/D boundary on combined biostratigraphy with any degree of confidence. It should be mentioned here that not all ammonoid workers have analyzed their samples for conodonts in the past and, conversely, conodont workers have not always reported ammonoid occurrences in their sampled sections.

SYSTEMATIC PALEONTOLOGY

Systematic descriptions are mainly based on the classification scheme of Tozer (1981, 1994), but modifications by Ware et al. (2018a, b) are incorporated. Morphological measurements are expressed using the four classic geometrical parameters of the shell: diameter (D), whorl height (H), whorl width (W) and umbilical diameter (U). Absolute values of H, W and U are plotted versus diameter, as are the ratios H/D, W/D and U/D. Terminology used to express shell size, umbilical width and type of coiling (whorl involution) is taken from Haggart (1989, table 8.1). All specimens are deposited in the New Mexico Museum of Natural History and Science (NMMNH) in Albuquerque.

Nearly all specimens were scanned using X-ray computed tomography (inspeXio SMX-225CT FPD HR, Shimadzu) at the National Museum of Nature and Science, Tsukuba, Japan

with settings of 0.01-0.05 mm resolution, 225 kV and 70 uA, and their whorl cross sections were drawn from the X-ray CT images.

Class CEPHALOPODA Cuvier, 1797
Superorder AMMONOIDA Hoffmann, 2022

Order CERATITIDA Hyatt, 1884

Superfamily MEEKOCERATOIDEA Waagen, 1895

Family OPHICERATIDAE Arthaber, 1911

Genus *Ghazalaites* Ware and Bucher, 2018a

Type species: *Ghazalaites roohiae* Ware and Bucher, 2018a

***Ghazalaites roohiae* Ware and Bucher, 2018a**

Figure 6A-F

1978 *Lytphiceras* sp. ind., Guex, pl. 1, fig. 4.

2018a *Ghazalaites roohii* Ware and Bucher, p.38, text-fig. 15, pl. 2, figs. 12-24.

2018b *Ghazalaites roohii* Ware and Bucher, p. 195, pl. 1, figs. 1-7, fig. 17.

2023b *Ghazalaites roohii* Ware and Bucher 2018a; Dai et al., figs. 6, 8, 10, 17.

Material: One measureable specimen (P-97301) from bed L-13555.

Description: Present specimen (P-97301): Very small sized (D=29 mm), very involute, compressed (W/D=0.26) immature shell with convex flanks that gently converge to a rounded venter without distinct shoulders. Whorl section sub-rectangular with maximum width at ~1/3 to 1/2 of flank height. Flank tapers very gradually from point of maximum width to a very narrow umbilicus (U/D=0.09) with abruptly rounded shoulder and low, near vertical wall. Umbilicus exhibits beginning stages of umbilical egression for which mature shells are known. No visible ornamentation on present specimen. Suture line with relatively low saddles and shallow lobes. Third lateral saddle somewhat asymmetric with dorsal side grading into unusually long auxiliary series characterized by numerous indentations.

Measurements: See Table 1.

Taxonomic Note: The ammonoid *Ghazalaites roohiae* Ware and Bucher 2018a, which was named after Ghazala Roohi of the Pakistan Museum of Natural History, was mistakenly given a Latinized species name that did not agree with the honoree's gender, i.e., *G. roohii*. This oversight is herein corrected according to ICZN Article 34.2 to agree with rule 31.1.

Discussion: *Ghazalaites roohiae* is a relatively new taxon from the Salt Range whose range of intraspecific variation is well defined by its unusually large sample, i.e., 47 specimens (Ware et al., 2018a). Its most distinguishing feature is the remarkable amount of umbilical egression exhibited by its larger, mature shells. Indeed, even though the present specimen is an immature shell, its coiling, as indicated by the umbilical seam at the end of the ultimate whorl, is already becoming egressive. Most of the illustrated shells from the Salt Range bear very weak but obvious prosiradiate, sigmoidal folds that become slightly stronger towards the aperture. In addition, as the conch becomes larger the point of maximum whorl width shifts slightly towards the center, and the umbilical shoulder gradually becomes indistinct with a corresponding oblique wall (Ware et al., 2018a). The suture line of the present specimen bears an obvious similarity to that illustrated by Ware et al. (2018a), especially the shape of the saddles and lobes as well as the unusually long auxiliary series. These observed similarities leave little doubt about the attribution of the present specimen to *G. roohiae*.

Occurrence: The measured specimen (P-97301) was found in bed L-13555 in the Crittenden Springs-north section (Figs. 2A, 3).

Family GYRONITIDAE Waagen, 1895

Genus *Gyronites* Waagen, 1895

Type species: *Gyronites frequens* Waagen, 1895

***Gyronites rigidus* (Diener, 1897)**

Figure 6G-I"

1897 *Danubites rigidus* Diener, pp. 36, 37, pl. 15, figs. 4 (lectotype), 5.

?1909 *Xenodiscus* cf. *plicosus* (Waagen, 1895); von Krafft & Diener, pp. 101, 102, pl. 25, fig. 4.

2018a *Gyronites rigidus* (Diener, 1897); Ware et al., pp.45, 46, text-fig. 16, pl. 5, figs. 1-3.

2023b *Gyronites rigidus* (Diener, 1897); Dai et al., figs. 6, 8, 10, 17, 19.

Material: 25 measured specimens ranging in diameter from 9.3 to 35.5 mm. Two specimens (P-97259, P-97260) from locality L-13552. Four specimens (P-97261, P-97262, P-97263 and P-97264) from float locality L-13553. Nine specimens (P-97265, P-97266, P-97267, P-97268, P-97269, P-97270, P-97271, P-97272 and P-97273) from locality L-13555. Three specimens (P-97274, P-97275 and P-97276) from locality L-13554. Seven specimens (P-97277, P-97278, P-97279, P-97280, P-97281, P-97282 and P-97283) from locality L-13556. See Table 1.

Description: Very small (avg. D = 18.0 mm), fairly evolute, moderately compressed shell (W/D = 0.24; W/H = 0.65) with slightly convex flanks, very angular ventral shoulders, wide tabulate venter and ovate whorl section with maximum width at ~mid-flank. Lower portion of convex flank gradually merges with preceding whorl, without discernable wall or shoulder, forming a moderately wide (U/D=0.38), very shallow umbilicus. Ornamentation consists of distant, slightly rursiradiate, fold-type ribs arising just above umbilical seam and fading away high on flank just below ventral shoulder. Ribbing frequency generally quite dense on early whorls, becoming more distant on outer whorl. Strength of ribbing highly variable from specimen to specimen, ranging from smooth to barely perceptible to very obvious. Suture line fairly simple and typical of *Gyronites*, with weakly indented 1st lateral lobe. Second lateral saddle larger than first.

Measurements: See Table 1 and Fig. 7.

Discussion: The fairly evolute, compressed specimens from Crittenden Springs, with their ovate whorl section, wide tabulate venter, non-discernable umbilical wall and frequency and style of ribbing, fit quite well within *Gy. rigidus*. They differ significantly from other early Dienerian gyronitids, i.e., *Gy. dubius* with its distinctive sub-trapezoidal whorl section, *Gy. plicosus* with its slightly more evolute shell, wider conch and high, almost vertical umbilical wall on robust variants, which moves the maximum whorl width to just slightly above the umbilical shoulder, *Gy. sitala* by its significantly more evolute shell, and *Gy. subdharmus*, mainly by its low, yet distinctive, nearly vertical umbilical wall. *Gyronites rigidus* differs from *Gy. frequens* by its much smaller size (avg. D = 18.0 mm vs. 32.2 mm), and, as shown on the box plot comparison (Fig. 10), *Gy. rigidus* differs from *Gy. frequens* by its slightly more evolute coiling (U.D = 0.37 vs. 0.32) and its slightly more robust whorl section (W/D = 0.24 vs. 0.21).

Occurrence: *Gyronites rigidus* occurs in each of the four lowest, fossiliferous beds, i.e., L-13552, L-13555, L-13554 and L-13556, as well as float locality L-13553, in the Crittenden Springs-north section (Figs. 2A, 3).

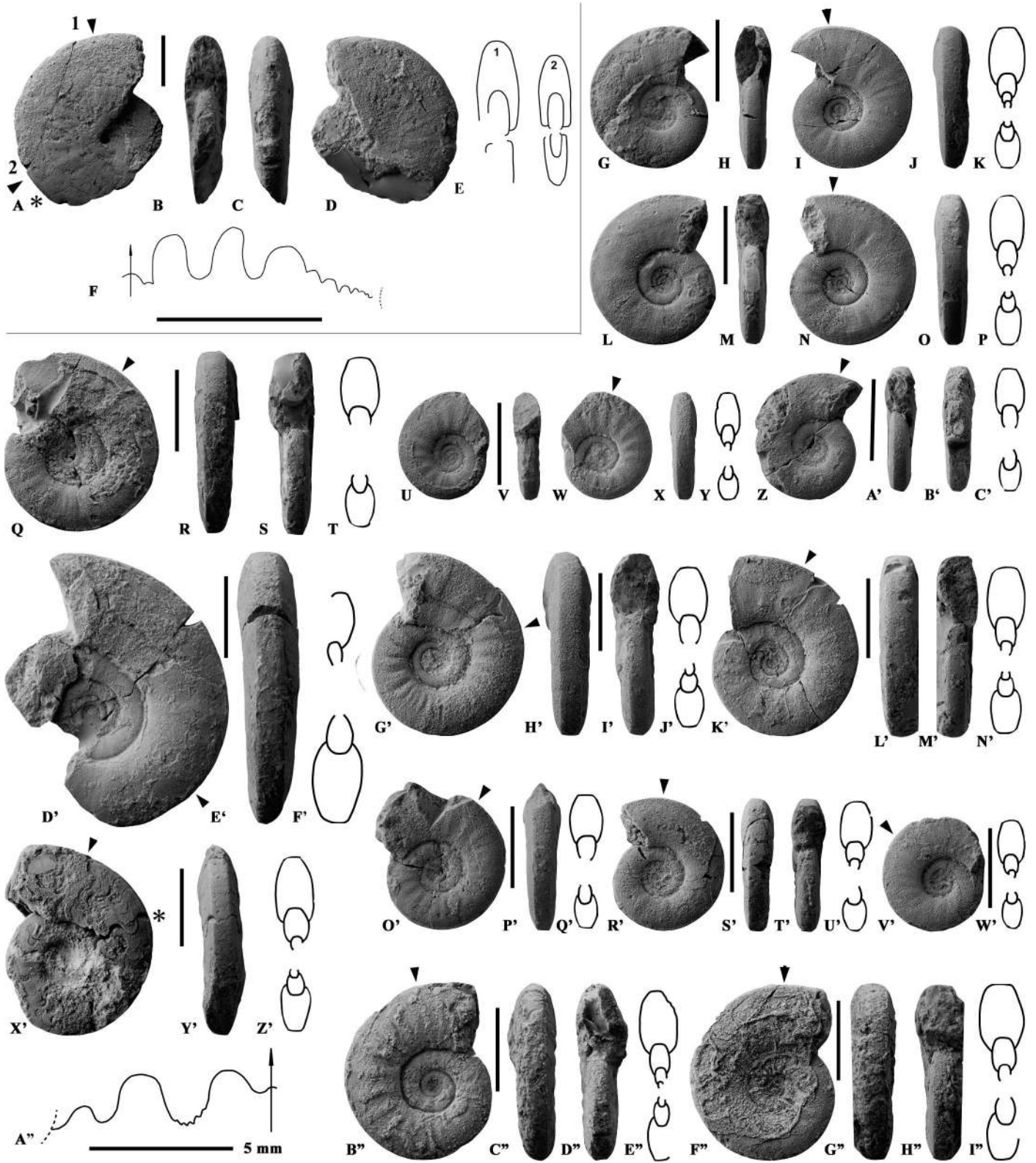


FIGURE 6 (facing page). **A-F**, *Ghazalaites roohiae* Ware et al., in **A-F**, P-97301, L-13555, in **A**, left lateral, **B**, apertural, **C**, ventral and **D**, right lateral views. **E**, whorl cross sections. **F**, suture line, H=15 mm. **G-I'**, *Gyronites rigidus* (Diener), P-97277, L-13556, in **G**, left lateral, **H**, apertural, **I**, right lateral and **K**, whorl cross section. **L-P**, P-97280, L-13556, in **L**, left lateral, **M**, apertural, **N**, right lateral and **O**, ventral views. **P**, whorl cross section. **Q-T**, P-97282, L-13556, in **Q**, lateral view, **R**, ventral, **S**, apertural views and **T**, whorl cross section. **U-Y**, P-97278, L-13556, in **U**, left lateral, **V**, apertural, **W**, right lateral, and **X**, ventral views. **Y**, whorl cross section. **Z-C'**, P-97281, L-13556, in **Z**, lateral, **A'**, apertural, and **B'** ventral views. **C'**, whorl cross section. **D'-F'**, P-97274, L-13554, in **D'**, lateral and **E'**, ventral views. **F'** whorl cross section. **G'-J'**, P-97266, L-13555, in **G'**, lateral, **H'**, ventral, and **I'**, apertural views. **J'**, whorl cross section. **K'-N'**, P-97267, L-13555, in **K'**, lateral, **L'**, ventral and **M'**, apertural views. **N'**, whorl cross section. **O'-Q'**, P-97265, L-13555, in **O'**, lateral and **P'**, ventral views. **Q'**, whorl cross section. **R'-U'**, P-97273, L-13555, in **R'**, lateral, **S'**, ventral and **T'**, apertural views. **U'**, whorl cross section. **V'-W'**, P-97268, L-13555, in **V'**, lateral view and **W'**, whorl cross section. **X'-A''**, P-97264, L-13553, in **X'**, lateral and **Y'**, ventral views and **Z'**, whorl cross section. **A''**, suture line, H = 7.5 mm. **B''-E''**, P-97259, L-13552, in **B''**, lateral, **C''**, ventral and **D''**, apertural views. **E''**, whorl cross section. **F''-I''**, P-97260, L-13552, in **F''**, lateral, **G''**, ventral and **H''**, apertural views. **I''**, whorl cross section. All whorl cross sections from CT scan images, as indicated by position of black arrows in lateral views. All suture lines as indicated by asterisk in lateral views. All scale bars = 1 cm unless otherwise indicated.

Gyronites frequens Waagen, 1895

Figure 8A-X

- 1895 *Gyronites frequens* n. gen., n. sp. Waagen, pp. 292-294, pl. 38, figs 1, 2 (lectotype), 3, 4, pl. 40, fig. 4.
 1895 *Gyronites nangaensis* n. gen., n. sp. Waagen, pp. 297-298, pl. 37, fig. 5 (holotype).
 1895 *Lecanites psilogyrus* n. sp. Waagen, pp. 280, 281, pl. 39, fig. 5 (holotype).
 1895 *Lecanites undatus* n. sp. Waagen, pp. 281, 282, pl. 38, figs 1 (lectotype), 2.
 1895 *Prionolobus compressus* n. gen., n. sp. Waagen, pp. 313-315, pl. 35, fig. 3 (holotype).
 1895 *Prionolobus plicatus* n. gen., n. sp. Waagen, pp. 315-316, pl. 35, fig. 2 (holotype).
 1895 *Prionolobus plicatilis* n. gen., n. sp. Waagen, pp. 318, 319, pl. 36, fig. 1 (holotype).
 ?1909 *Xenodiscus lilangensis* n. sp. von Krafft & Diener, pp. 97-99, pl. 25, figs. 6-10.
 1909 *Xenodiscus khoorensis* n. sp. von Krafft & Diener, p. 88.
 1934 *Gyronites frequens* Waagen, 1895; Spath, pp. 91, 92, fig. 19 [cop. Waagen, 1895].
 ?1976 *Gyronites psilogyrus* Waagen, 1895; Wang & He, p. 274, fig. 71, pl. 1, figs. 9, 10.
 ?1976 *Prionolobus plicatilis* Waagen, 1895; Wang & He, p. 275, fig. 8a, pl. 3, figs. 13-15.
 v1978 *Gyronites frequens* Waagen, 1895; Guex, pl. 1, fig. 3.
 v1978 *Gyronites undatus* Waagen, 1895; Guex, pl. 8, fig. 3.
 ?1996 *Gyronites frequens* Waagen, 1895; Waterhouse, pp. 33, 34, text-fig. 4A, pl. 1, figs. 1-4.
 ?1996 *Gyronites planissimus* Koken, 1934; Waterhouse, pp. 34, 35, text-fig. 4A, pl. 1, figs. 5, 8.
 ?1996 *Gyronites spiralis* n. sp. Waterhouse, pp. 35, 36, text-fig. 4A, pl. 1, figs. 6, 7, 9, 10.
 non v2008 *Gyronites frequens* Waagen, 1895; Brühwiler et al., p. 1168, pl. 5, figs. 7, 8 (= *Ambites bjerageri* Ware and Bucher 1918).
 2018a *Gyronites frequens* Waagen, 1895; Ware et al., pp. 41-44, text-figs. 16-18, pl. 3, figs. 1-5, pl. 4, figs. 1-17.
 2018b *Gyronites frequens* Waagen, 1895; Ware et al., pp. 195-196, text-fig. 18, pl. 1, figs. 8-18.
 2023b *Gyronites frequens* Waagen, 1895; Dai et al., figs. 8, 13C, 17, 19.

Material: Eleven measured specimens ranging in diameter from 26.3 to 50.4 mm. One specimen (P-97284) from locality L-13557. Eight specimens (P-97285, P-97286, P-97287, P-97288, P-97289, P-97290, P-97291 and P-97292) from locality L-13558. Two specimens (P-97293, P-97294) from locality L-13559. In addition, one unmeasurable specimen (P-97589 from L-13588) consisting only of a body chamber fragment, if complete, would have measured approximately 60 mm in diameter.

Description: Fairly small (avg. D = 32.1), fairly evolute, very compressed shell (W/D = 0.21, W/H = 0.49) with convex flanks, angular ventral shoulders, wide tabulate venter and thin ovate whorl section with maximum width at ~mid flank. Lower portion of convex flank gradually merges with preceding whorl at a very obtuse angle (~135°), without discernable wall or shoulder, forming a moderately wide (U/D = 0.30), very shallow umbilicus. Ornamentation not preserved on most of the studied specimens due to poor preservation, but one specimen (3087C) exhibits barely perceptible, fairly dense, and radial to slightly prosiradiate ribs that arise on umbilical shoulders of inner whorls, traverse across the flank and fade before reaching ventral shoulder. Ribs appear to fade on outer whorl. Specimen P-97285 exhibits same style of ribbing but much weaker, and faint growth lines are also present. Suture line fairly simple and typical of *Gyronites*, with second lateral saddle larger than first. Lobes and saddles definitely not as deep and elongated as those of the specimen illustrated by Ware et al. (2018a, pl. 4, fig. 17).

Measurements. See Table 1 and Fig. 9

Discussion: This taxon is not as plentiful at Crittenden Springs as *Gy. rigidus*, and its preservation tends to be considerably worse. Nevertheless, based on their much larger size and more involute coiling, we are confident that the specimens are properly attributed to *Gy. frequens*. According to Ware et al. (2018a), the relatively large number of well-preserved specimens amassed from the Salt Range (111) enabled them to thoroughly describe the taxon's wide range of intraspecific variability. One key diagnostic feature they recognized is the taxon's allometric growth pattern; that is, the shells become more evolute with increasing diameter. We are unable to recognize this feature in our material due to the relatively low number of specimens combined with their generally poor preservation.

Occurrence: *Gyronites frequens* occurs in each of the three highest fossiliferous beds, i.e., L-13557, L-13558 and L-13559, in the Crittenden Springs (north) section (Figs. 2A, 3).

Gyronites bullatus Ware et al. 2018b

Figure 8Y-D'

- 2018b *Gyronites bullatus* n. sp. Ware and Bucher, p. 197, pl. 2, figs. 22-28.
 2023b *Gyronites bullatus* Ware and Bucher, 2018b; Dai et al., fig. 19.

Material: Two measured specimens (P-97295 P-97296) from locality L-13559.

Description: Very small (avg. D = 27.9 mm), very evolute, very compressed shell (W/D = 0.21, W/H = 0.60) with convex flanks convergent upon abruptly rounded ventral shoulders, tabulate venter and ovate inner whorl that transitions to sub-trapezoidal outer whorl section with maximum width at ~40% of whorl height. Lower portion of convex flank meets with preceding whorl at a fairly obtuse angle (~110°) forming a fairly wide, shallow umbilicus (U/D = 0.41) without discernable wall

TABLE 1. Measurements, Early Dienerian ammonoids from Crittenden Springs- north area.

EARLY DIENERIAN AMMONOIDS FROM CRITTENDEN SPRINGS- NORTH AREA (all measurements from CT scan images unless otherwise indicated by asterisk)										
NMMNH P-	Taxon	NMMNH L-	D _{mm}	W	H	U	W/D	H/D	U/D	W/H
97259	<i>Gyronites rigidus</i>	13552	22.0	4.8	8.0	8.2	0.22	0.36	0.37	0.60
97260	<i>Gyronites rigidus</i>	13552	21.6	5.3	8.2	7.6	0.25	0.38	0.34	0.63
97261	<i>Gyronites rigidus</i>	13553	11.9	3.4	5.2	4.3	0.28	0.43	0.36	0.65
97262	<i>Gyronites rigidus</i>	13553	25.3	5.9	9.4	9.3	0.23	0.37	0.37	0.62
97263	<i>Gyronites rigidus</i>	13553	18.5	4.8	7.3	6.3	0.26	0.39	0.34	0.66
97264	<i>Gyronites rigidus</i>	13553	11.3	3.2	4.1	4.1	0.29	0.37	0.37	0.78
97265	<i>Gyronites rigidus</i>	13555	16.6	4.1	6.0	6.5	0.25	0.36	0.39	0.68
97266	<i>Gyronites rigidus</i>	13555	19.6	4.6	6.9	7.6	0.24	0.35	0.39	0.67
97267	<i>Gyronites rigidus</i>	13555	21.6	4.8	8.1	8.0	0.22	0.38	0.37	0.60
97268	<i>Gyronites rigidus</i>	13555	13.8	3.3	5.4	4.7	0.24	0.39	0.34	0.62
97269*	<i>Gyronites rigidus</i>	13555	18.4	4.6	6.6	7.4	0.25	0.36	0.40	0.70
97270	<i>Gyronites rigidus</i>	13555	16.4	3.9	6.1	5.9	0.24	0.38	0.36	0.64
97271*	<i>Gyronites rigidus</i>	13555	11.6	3.1	4.4	4.6	0.27	0.38	0.40	0.70
97272*	<i>Gyronites rigidus</i>	13555	9.3	2.4	3.4	3.4	0.26	0.37	0.37	0.71
97273*	<i>Gyronites rigidus</i>	13555	16.2	4.0	5.9	6.5	0.25	0.36	0.40	0.68
97274	<i>Gyronites rigidis</i>	13554	27.8	5.8	9.8	11.3	0.21	0.35	0.41	0.59
97275	<i>Gyronites rigidis</i>	13554	35.5	7.7	11.5	15.2	0.22	0.32	0.43	0.67
97276	<i>Gyronites rigidis</i>	13554	25.0	5.0	8.9	9.9	0.20	0.35	0.39	0.56
97277	<i>Gyronites rigidus</i>	13556	17.7	4.5	7.2	6.0	0.25	0.41	0.34	0.63
97278	<i>Gyronites rigidus</i>	13556	13.0	3.0	5.1	4.5	0.23	0.39	0.35	0.58
97279*	<i>Gyronites rigidus</i>	13556	10.9	2.9	4.3	3.8	0.27	0.39	0.35	0.67
97280	<i>Gyronites rigidus</i>	13556	18.1	4.0	6.7	6.7	0.22	0.37	0.37	0.60
97281	<i>Gyronites rigidus</i>	13556	16.6	3.8	6.2	6.3	0.23	0.37	0.38	0.62
97282	<i>Gyronites rigidus</i>	13556	20.7	4.6	7.4	8.0	0.22	0.36	0.39	0.63
97283*	<i>Gyronites rigidus</i>	13556	9.7	2.8	3.5	3.8	0.29	0.36	0.39	0.80
97284	<i>Gyronites frequens</i>	13557	39.2	-	15.4	12.0	-	0.39	0.31	-
97285	<i>Gyronites frequens</i>	13558	50.4	-	18.8	17.3	-	0.37	0.34	0.34
97286	<i>Gyronites frequens</i>	13558	26.6	5.1	9.9	9.2	0.19	0.37	0.35	0.52
97287	<i>Gyronites frequens</i>	13558	26.3	5.3	9.5	9.7	0.20	0.36	0.37	0.56
97288*	<i>Gyronites frequens</i>	13558	37.3	7.3	15.1	10.0	0.20	0.40	0.27	0.48
97289	<i>Gyronites frequens</i>	13558	35.5	6.5	13.9	12.0	0.18	0.39	0.34	0.47
97290	<i>Gyronites frequens</i>	13558	15.8	4.0	7.6	3.4	0.25	0.48	0.22	0.53
97291*	<i>Gyronites frequens</i>	13558	42.0	8.9	15.3	13.4	0.21	0.36	0.32	0.58
97292*	<i>Gyronites frequens</i>	13558	39.9	7.5	13.6	16.9	0.19	0.34	0.42	0.55
97293	<i>Gyronites frequens</i>	13559	17.5	4.0	8.0	4.2	0.23	0.46	0.24	0.51
97294*	<i>Gyronites frequens</i>	13559	23.1	5.8	9.0	7.8	0.25	0.39	0.34	0.64
97589**	<i>Gyronites frequens</i>	13558	~60	-	-	-	-	-	-	-
97295	<i>Gyronites bullatus</i>	13559	27.3	5.6	9.5	11.2	0.21	0.35	0.41	0.59
97296*	<i>Gyronites bullatus</i>	13559	28.5	5.9	9.6	10.9	0.21	0.34	0.38	0.61

97297	<i>Ussuridiscus varaha</i>	13553	-	10.4	25.3	4.0	-	-	-	0.41
97298	<i>Ussuridiscus varaha</i>	13555	-	10.7	25.3	4.8	-	-	-	0.43
	(penultimate whorl)	13555	24.4	5.7	13.3	2.1	0.23	0.54	0.09	0.43
97299	<i>Ussuridiscus varaha</i>	13554	74.5	16.5	37.7	10.2	0.22	0.51	0.14	0.44
97300	<i>Ussuridiscus varaha</i>	13556	28.9	6.0	15.7	2.1	0.21	0.61	0.07	0.38
97301*	<i>Ghazalaites roohiae</i>	13555	28.6	7.5	15.7	2.5	0.26	0.55	0.09	0.48
97302	<i>Proptychites</i> sp.	13558	28.8	10.3	14.0	5.7	0.36	0.49	0.20	0.74
97303	Gen et sp. indet.	13553	12.3	3.2	5.1	3.2	0.26	0.41	0.25	0.61

* Indicates measurements by hand.

** Specimen not measurable.

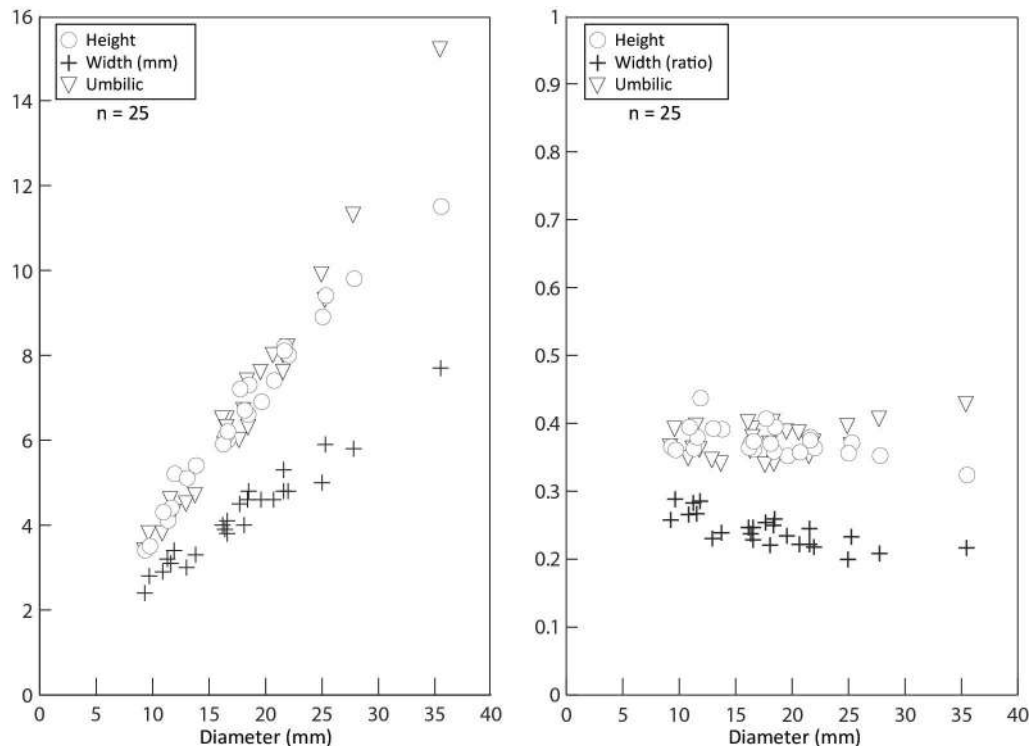


FIGURE 7. Scatter diagram comparison of H, W and U, and H/D, W/D and U/D for *Gyronites rigidus*.

or shoulder. Ornamentation consists of fairly dense, slightly prosiradiate ribs that arise on umbilical shoulder and form weak bullae at mid-flank before fading near ventral shoulder. Ribs tend to lose bullae feature and become denser and weaker on outer whorl. Suture line not preserved on present specimens, but according to Ware et al. (2018b), suture line of specimens from Spiti is typical of *Gyronites*, with “second lateral saddle larger than the others, lobes with a few small indentations and no auxiliary series”.

Measurements: See Table 1.

Discussion: *Gyronites bullatus* is similar in size and morphology to *Gy. rigidus*, but it is slightly more compressed and evolute, and it differs from *Gy. frequens* by its smaller size, more evolute coiling and slightly more robust whorl section. According to Ware et al. (2018b), the inner whorls of this taxon exhibit a “rather high and vertical umbilical wall” that transitions to a more oblique wall on the body chamber. This feature is not present on our two specimens. Also, the ribbing

style on the body chamber of the only specimen with ribs (P-97295) differs somewhat from *Gy. bullatus*. We conclude that these differences are nevertheless within the taxon’s range of intraspecific variation, especially since *Gy. bullatus* was erected based only on two specimens.

Occurrence: The two specimens of *Gy. bullatus* were found in bed L-13559 in the Crittenden Springs-north section (Figs 2A, 3).

Family PROPTYCHITIDAE Waagen, 1895

Genus *Proptychites* Waagen, 1895

Type species: *Ceratites lawrencianus* de Koninck, 1863

***Proptychites* sp.**

Figure 11Q-U

Material: One measured specimen (P-97302) from locality L-13558.

Description: Present specimen: Fairly small (D = 28.8 mm), fairly involute, fairly compressed (W/H=0.74) shell with

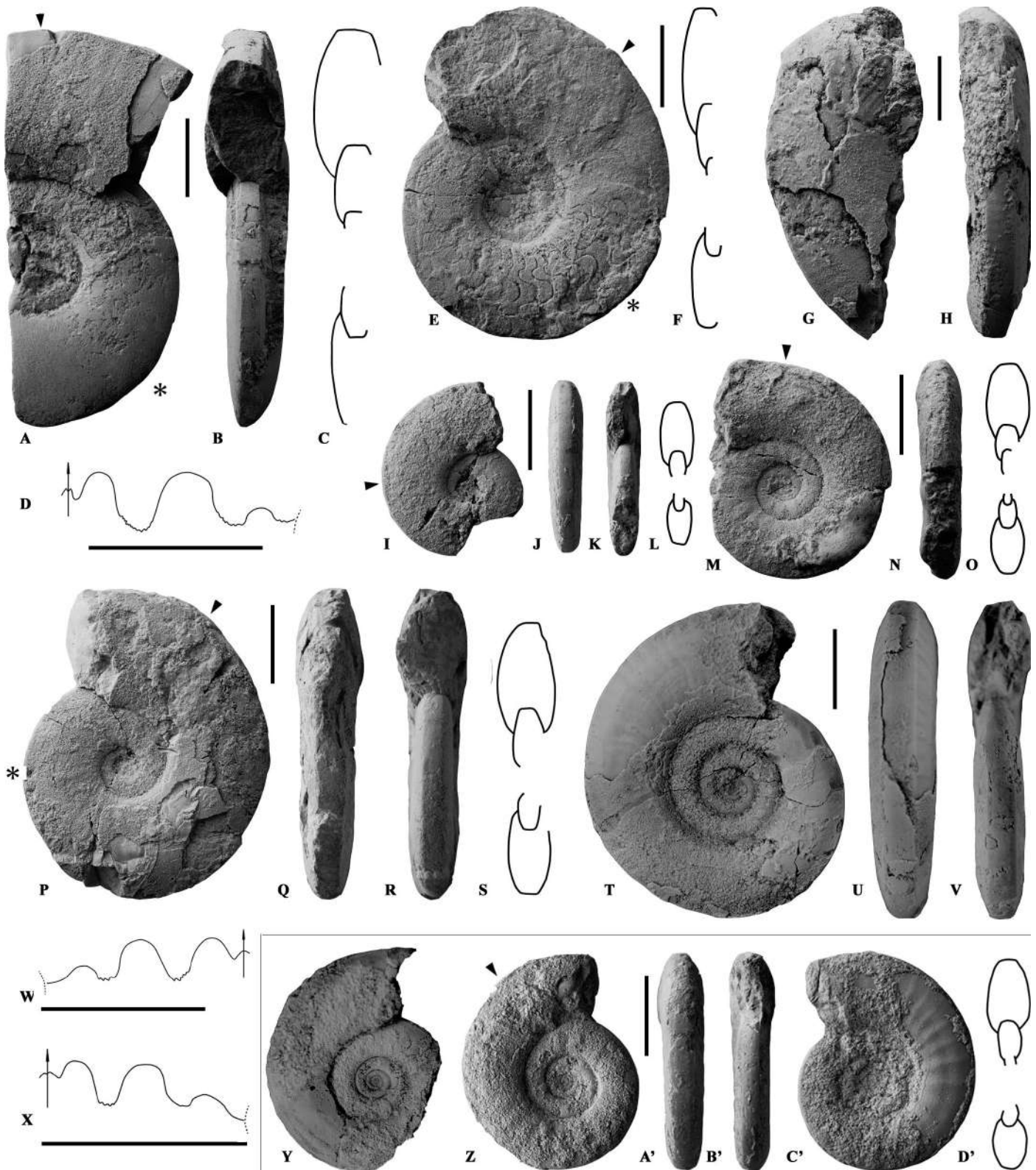


FIGURE 8. A-X, *Gyronites frequens* Waagen, in A-D, P-97285, L-13558, in A, lateral and B, apertural views. C, whorl cross section. D, suture line, H=13 mm. E-F, W, P-97284, L-13557, in E, lateral, F, whorl cross section and W, suture line, H=12 mm. G-H, P-97589, L-13558, large body chamber fragment (not measureable), in G, lateral and H, ventral views. I-L, P-97293, L-13559, in I, lateral, J, ventral and K, apertural views. L, whorl cross section. M-O, P-97287, L-13558, in M, lateral and N, ventral views. O, whorl cross section. P-S, X, P-97290, L-13558, in P, lateral, Q, ventral and R, apertural views. S, whorl cross section. X, suture line, H=9.7 mm. T-V, P-97292, L-13558, in T, lateral, U, ventral and V, apertural views. Y-D', *Gyronites bullatus* Ware et al., in Y, P-97296, L-13559, lateral view. Z-D', P-97295, L-13559, in Z, left lateral, A', ventral, B', apertural and C', right lateral views. D', whorl cross section. All whorl cross sections from CT scan images, as indicated by position of black arrows in lateral views. All suture lines as indicated by asterisk in lateral views. All scale bars = 1 cm.

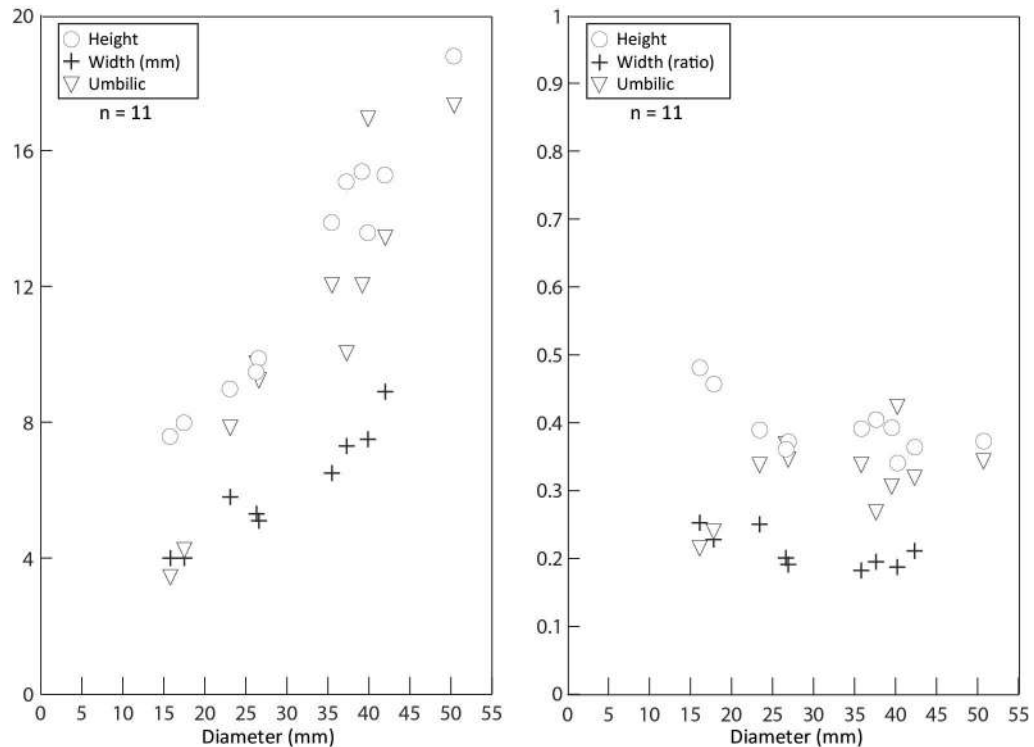


FIGURE 9. Scatter diagram comparison of H, W and U, and H/D, W/D and U/D for *Gyronites frequens*.

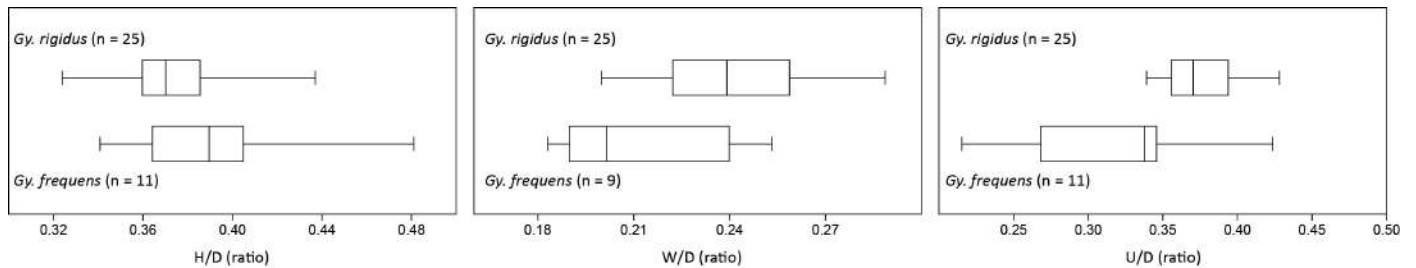


FIGURE 10. Box plot comparison of H/D, W/D and U/D for *Gy. rigidus* vs. *Gy. frequens*.

broadly rounded venter. Whorl section transitions from sub-triangular with maximum width at top of umbilical shoulder on inner whorls to more broadly ovate with maximum width at ~40% of flank height on outer whorl. Umbilicus fairly narrow (U/D=0.20) with relatively low, steep to vertical wall and narrowly rounded shoulder. No visible ornamentation. Suture line very simple with broad 1st and 2nd lateral saddles, and low, asymmetric third lateral saddle whose dorsal side grades into relatively long auxiliary series. Lobes with relatively few, small, weak indentations.

Measurements: See Table 1.

Discussion: Our specimen's whorl morphology is similar in a general sense to the type specimen of *Proptychites oldhamianus* Waagen, 1895, as well as to the specimens illustrated by Ware et al. (2018a, b) from the Salt Range and Spiti, respectively. However, the flanks of the present specimen are slightly more convex, its umbilical wall, while quite steep, is not vertical, and its venter is more broadly rounded. The venter at the beginning of the penultimate whorl (see image generated from CT scan, Figure 11T) appears to be more narrowly rounded, but this phenomenon is considered to be a result of preservational bias (slight distortion). Its suture line, while simple, is actually simpler than that of *P. oldhamianus*. Its saddles are much broader, the 1st lateral lobe is not near as deep and its indentations are very weak. In summary, more specimens are needed from Crittenden

Springs in order to make a species-level determination.

Occurrence: The present specimen was found in bed L-13558 in the Crittenden Springs-north section (Figs. 2A, 3)

Family MULLERICERATIDAE Ware et al., 2011

Genus *Ussuridiscus* Shigeta and Zakharov, 2009

Type species: *Ussuridiscus varaha* (Diener, 1895)

***Ussuridiscus varaha* (Diener, 1895)**

Figure 11A-P

1895 *Meekoceras* (*Kingites*) *varaha* n. sp. Diener, p. 52, pl. 1, fig.2. (holotype).

non 1897 *Kingites varaha* (Diener), 1895; Diener, pp. 143, 144, pl. 6, fig. 2, pl. 7, fig. 6.

1905 *Meekoceras* (*Kingites*) *varaha* Diener, 1895; Noetling, pl. 32, fig. 5 [cop. Diener, 1895].

non 1909 *Meekoceras varaha* (Diener, 1895); von Krafft & Diener, pp. 17-20, pl. 2, figs. 2-6, pl. 14, figs. 7, 8.

1968 *Koninckites varaha* (Diener, 1895; Zakharov, p. 91, text-fig. 20b, pl. 17, figs. 4, 5.

2007 *Hubeitoceras* (?) *wangi* n. sp. Zakharov & Mu, p. 871, figs. 13.17-13.19, 15.2-15.5.

v p 2008 '*Koninckites*' cf. *timorense* (Wanner, 1911); Brühwiler et al., pp. 1165-1166, pl. 3, figs. 1-4, pl. 4, fig. 1.

non v p 2008 '*Koninckites*' cf. *timorense* (Wanner, 1911); Brühwiler et al., pl. 4, fig. 2.

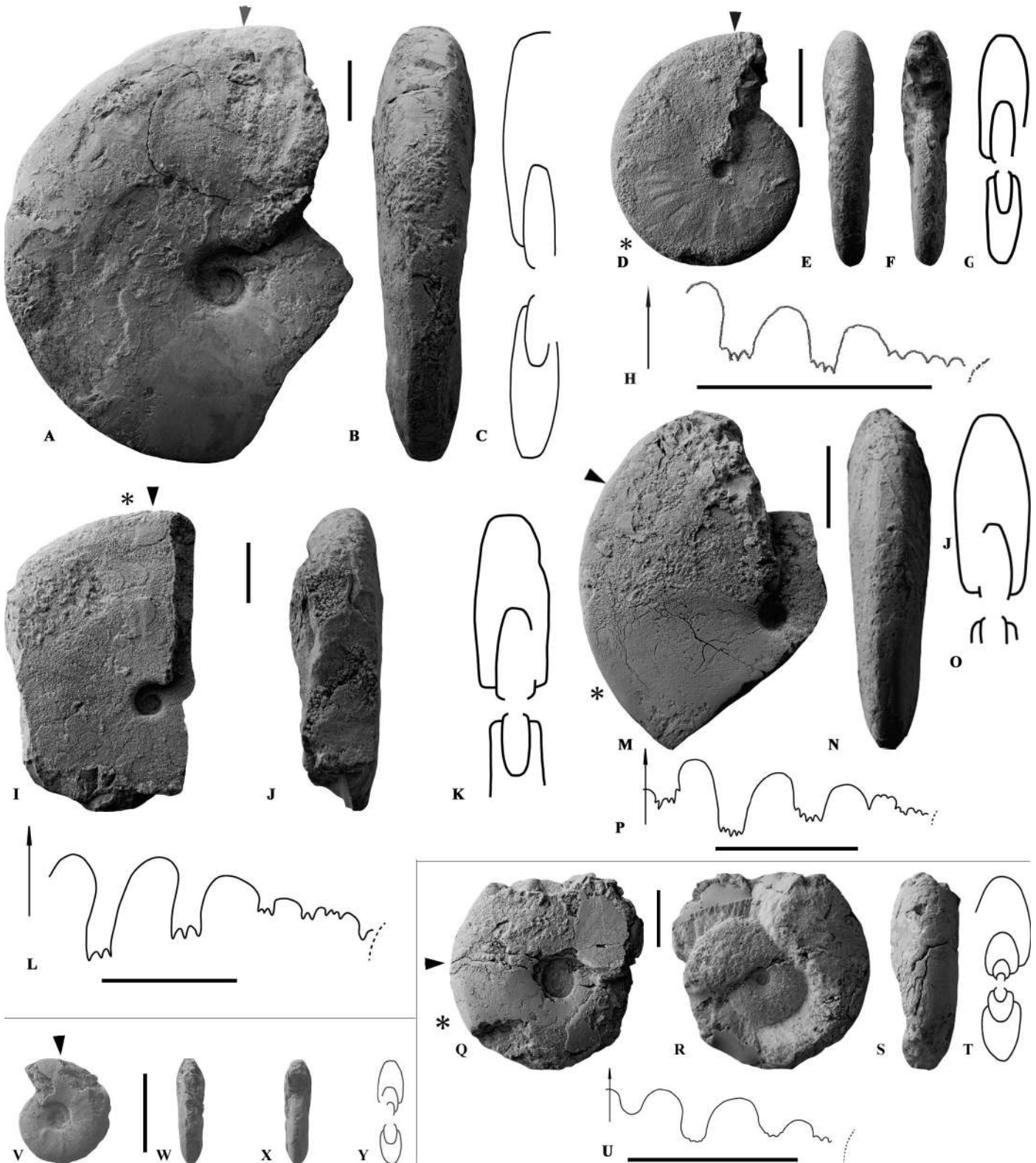


FIGURE 11. **A-P**, *Ussuridiscus varaha* (Diener), in **A-C**, P-97299, L-13554, in **A**, lateral and **B**, ventral views. **C**, whorl cross section. **D-H**, P-97300, L-13556, in **D**, lateral, **E**, ventral and **F**, apertural views. **G**, whorl cross section. **H**, suture line, H = 12.4 mm. **I-L**, P-97298, L-13555, in **I**, lateral and **J**, ventral views. **K**, whorl cross section. **L**, Suture line, H = 25.7 mm. **M-P**, P-97297, L-13553, in **M**, lateral and **N**, ventral views. **O**, whorl cross section. **P**, suture line, H = 20.8 mm. **Q-U**, *Proptychites* sp., P-97302, L-13558, in **Q**, right lateral, **R**, left lateral and **S**, ventral views. **T**, whorl cross section. **U**, suture line, H = 14.4 mm. **V-Y**, Gen. et sp. indet., P-97303, L-13553, in **V**, left lateral, **W**, ventral and **X**, apertural views. **Y**, whorl cross section. All whorl cross sections from CT scan images, as indicated by position of black arrows in lateral views. All suture lines as indicated by asterisk in lateral views. All scale bars = 1 cm.

- 2009 *Ussuridiscus varaha* (Diener, 1895); Shigeta & Zakharov, pp. 69-73, figs. 50.5, 50.6, 55-57.
 2018a *Ussuridiscus varaha* (Diener, 1895); Ware et al., p. 94, 95, pl. 28, figs. 19-31, figs. 49, 53.
 2018b *Ussuridiscus varaha* (Diener, 1895); Ware et al., p. 211, pl. 12, figs. 12, 13.
 2019 *Ussuridiscus* cf. *U. varaha* Shigeta and Zakharov, 2009; Dai et al., pp. 14-16, figs. 15.1-15.5, 15.8-15.18.
 2023b *Ussuridiscus varaha* (Diener, 1895); Dai et al., figs. 6, 8, 17, 19.

Material: Two measured specimens ranging in diameter from 29 mm to ~75 mm, and two additional but incomplete specimens. One specimen (P-97300) from bed L-13556. One specimen (P-97299) from bed L-13554. One specimen (P-97298) from bed L-13555. One specimen (P-97297) from locality L-13553.

Description: Smaller specimens: Fairly small ($D=29$ to ~44 mm), moderately involute, very compressed platycone ($W/D=0.22$, $W/H=0.41$) with very slightly convex flanks. Whorl section sub-rectangular with maximum width at ~50 to 65% of whorl height. Lower portion of flank very slightly convergent from point of maximum width to umbilical margin. Upper part of flank converges much more rapidly to a relatively narrow, subtabulate to tabulate venter with abruptly rounded shoulders. Umbilicus very narrow ($U/D=0.07$ to 0.14) with abruptly rounded shoulder and low, vertical wall. Two of the smaller specimens bear no visible ornamentation, but one specimen (P-97300) exhibits weak, fairly dense, slightly prosiradiate, fold type ribs that arise at about 25% of whorl height, gain maximum strength at mid-flank and fade high on flank well below ventral shoulder. Suture line ceratitic with deep first lateral lobe and asymmetric 2nd and 3rd lateral saddles; dorsal side of 3rd lateral saddle transitions into long auxiliary series with numerous indentations. Larger specimen ($D\approx 75$ mm): Moderately involute, very compressed platycone ($W/D=0.22$, $W/H=0.44$) with more convex flanks than smaller specimens. Whorl section sub-rectangular with maximum width at ~50% of height. Convexity between upper and lower halves of flank nearly identical. Venter subtabulate with abruptly rounded shoulders. Umbilicus narrow with broadly rounded shoulder and low wall that meets preceding whorl at fairly steep angle. No visible ornamentation. Suture line not preserved.

Measurements: See Table 1.

Discussion: The genus *Ussuridiscus* was erected by Shigeta and Zakharov (2009) with *Meekoceras* (*Kingites*) *varaha* Diener, 1895 as the type species. Prior to the present work, *U. varaha* was known only from the earliest Dienerian *Gyronites dubius* Zone of the Salt Range and Spiti (Ware et al., 2018a), and the late Griesbachian to early Dienerian *Gy. subdharmus* Zone of South Primorye (Shigeta and Zakharov, 2009). According to Shigeta and Zakharov (2009), *Ussuridiscus* is somewhat similar in morphology to *Radioceras* Waterhouse, 1996, *Kymatites* Waagen, 1895, and *Koninckites* Waagen, 1895 with regard to its involute shell and tabulate venter, but it can be distinguished by its overhanging umbilical wall. As per Ware et al. (2018a), it also bears some resemblance to *Mullericeras*, but can be differentiated from this genus by its simpler suture line, i.e., narrower ventral lobe and less numerous indentations in its lateral lobes. Ware et al. (2018a) assigned an additional species to *Ussuridiscus*, i.e., *U. ensanus* (von Krafft, 1909), and also erected two new species, i.e., *U. ventriosus* Ware et al. (2018a, based on only one specimen) and *U. ornatus* Ware et al. (2018a), all from the Salt Range. *Ussuridiscus varaha* clearly differs from *U. ensanus*, which is characterized by a sub-lanceolate whorl section and it differs from *U. ventriosus*, which features a thicker venter, vertical umbilical wall and suture line with a shorter auxiliary series. And, lastly, *U. varaha* differs from *U. ornatus* by the latter's particularly strong ribbing.

The present specimens match well in all aspects, i.e., general morphology, ornamentation and suture line, with those illustrated by Shigeta and Zakharov (2009) and Ware et al. (2018a), except that the slope of the umbilical wall appears to be vertical rather than overhanging. This minor discrepancy is considered to be the result of intraspecific variation.

Occurrence: Present specimens collected from beds L-13556, L-13554, L-13555 and float locality L-13553, in the Crittenden Springs-north section (Figs. 2A, 3)

Family OPHICERATIDAE Arthaber, 1911

Genus *Wordieoceras* Tozer, 1971

Type species: *Vishnuites wordiei* Spath, 1930

Wordieoceras wordiei (Spath) Tozer, 1971

Figure 12A-Y

- 1930 *Vishnuites wordiei* Spath, p. 31, pl. 2, figs. 11a, b (holotype)
 1930 *Vishnuites decipiens* Spath, p. 31, pl. 3, figs. 2a-g; pl. 4, figs. 2a, b.
 1935 *Vishnuites wordiei* Spath, p. 41, pl. 4, figs. 5a, b; pl. 12, figs. 2a, b
 1935 *Vishnuites decipiens* Spath, p. 41, pl. 4, figs. 4a, b; pl. 9, figs. 3a, b; pl. 10, figs. 2-5; pl. 12, figs. 1a, b; pl. 13, figs. 4, 7.
 1967 *Ophiceras decipiens* (Spath); Tozer, p. 16, 17, 51, 52 and 54.
 1971 *Wordieoceras wordiei* (Spath), Tozer p. 1031.
 1987 *Vishnuites domokhotovi* Zakharov and Rybalka, p. 36, pl. II, fig. 5
 1994 *Wordieoceras wordiei* (Spath); Tozer, p. 58, pl. 5, figs. 1-3; pl. 6, figs. 1-3; pl. 7, figs. 1-4.
 1996 *Wordieoceras decipiens* (Spath); Dagys and Ermakova, p. 416, pl. 11, figs. 1, 2, 4, 5.
 2006 *Wordieoceras wordiei* (Spath); Bjerager et al., p. 640, fig. 5.
 2006 *Wordieoceras decipiens* (Spath); Bjerager et al., p. 640, fig. 5, fig. 8, j-k; p. 644, 646.
 non 2007 *Wordieoceras* aff. *wordiei* (Spath); Mu et al., p. 862, figs. 6.7, 6.9, 6.11, 7.2, 7.2, 8.
 non 2009 *Wordieoceras* cf. *wordiei* (Spath); Shigeta and Zakharov, p. 68, pl. 50, figs. 12-15.
 2015 *Wordieoceras wordiei* (Spath); Jenks et al., p. 343, fig. 13.3, i-j., GSC28060.
 2021 *Wordieoceras wordiei* (Spath); Jenks et al., p. 11, figs. 7a-b'.
 2023b *Wordieoceras wordiei* (Spath); Dai et al., p. 36, fig. 22.

Material: Eight measured specimens (P-97304, P-97305, P-97306, P-97307, P-97308, P-97309, P-97310, and P-97311) consisting of complete phragmocones and partially complete, undistorted body chambers ranging in diameter from 28.3 to 74.7 mm. All specimens from L-13032. Specimens P-97304 and P-97311 exhibit nearly complete, undistorted body chambers.

Description: Small to medium sized, fairly evolute, compressed shell with convex flanks that converge gently to highly variable venter with/without distinct shoulders. Whorl section varies from sub-trigonal to ovoid to sub-rectangular on body chamber of some larger specimens; maximum whorl width occurs at ~35 to 45% of whorl height. Venter varies from nearly acute to fastigate with distinct bordering shoulders to narrowly rounded to more broadly rounded on body chambers of some larger specimens. Umbilicus moderately wide (U/D avg. 0.31) and fairly shallow with low, moderately to steeply inclined wall and shoulders that vary from barely perceptible to broadly rounded on some specimens to slightly more angular on others. No visible ornamentation (ribbing) on present specimens-test has been corroded away, but one specimen (P-97311) exhibits fairly dense, slightly forward projected growth lines on interior mold of the body chamber. Suture line typical for ophiceratids, with deep first lateral lobe and relatively high median saddle.

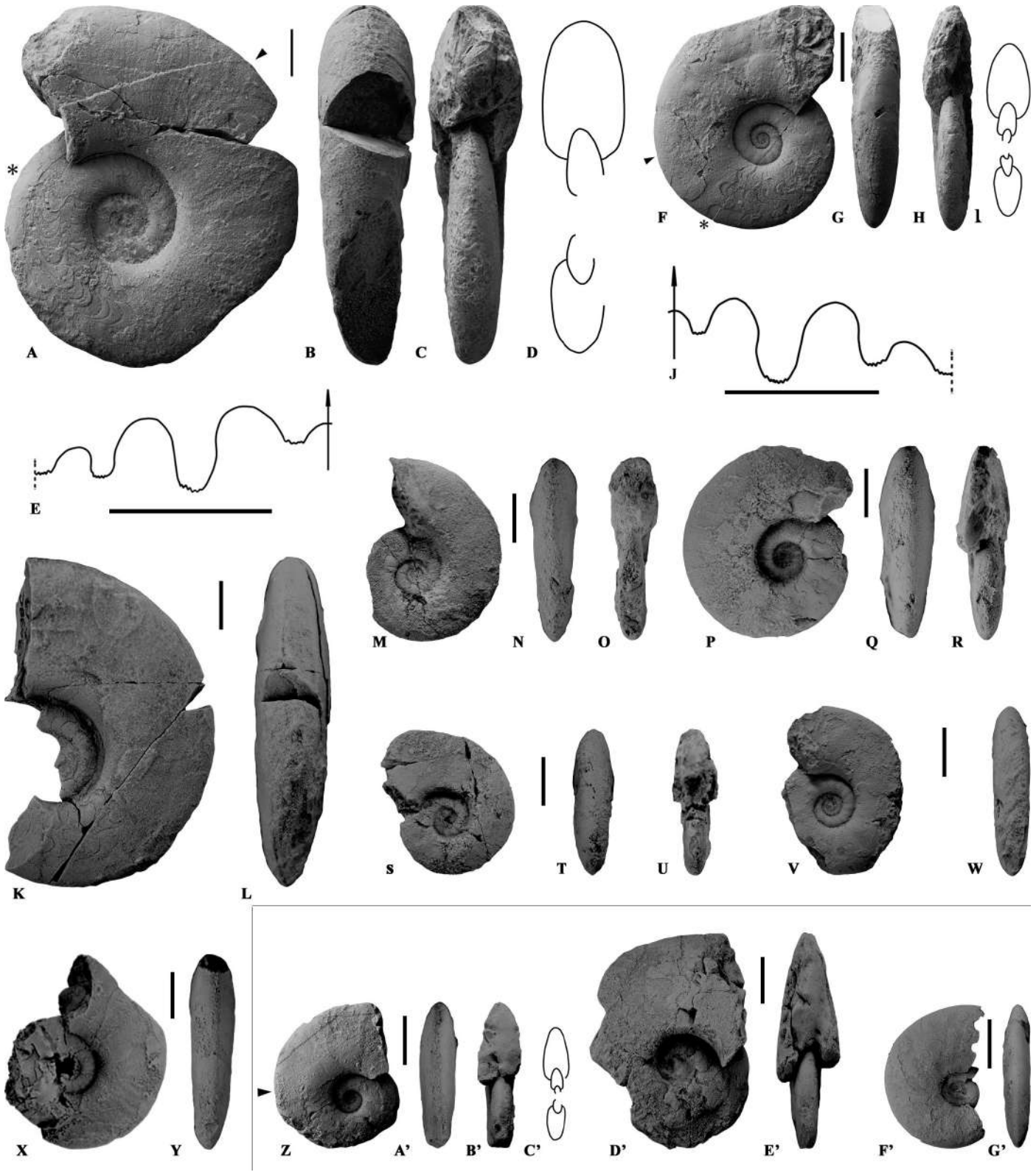


FIGURE 12. A-Y, *Wordieoceras wordiei* (Spath). A-E, P-97311, L-13032, in A, lateral, B, ventral and C, apertural views. D, whorl cross section. E, suture line, H=18.2 mm. F-J, P-97304, L-13032, in F, lateral, G, ventral and H, apertural views. I, whorl cross section. J, suture line, H= 18.0 mm. K-L, P-97310, L-13032, in K, lateral and L, ventral views. M-O, P-97308, L-13032, in M, lateral, N, ventral and O, apertural views. P-R, P-97305, L-13032, in P, lateral, Q, ventral and R, apertural views. S-U, P-97307, L-13032, in S, lateral, T, ventral and U, apertural views. V-W, P-97306, L-13032, in V, lateral and W, ventral views. X-Y, P-97309, L-13032, in X, lateral and Y, ventral views. Z-G', *Wordieoceras mullenae* Jenks et al., in Z-C', P-97313, L-13032, in Z, lateral, A', ventral and B' apertural views. C', whorl cross section. D'-E', P-97314, L-13032, in D', lateral and E' apertural views. F'-G', P-97312, L-13032, in F', lateral and G', ventral views. All whorl cross sections from CT scan images, as indicated by position of black arrows in lateral views. All suture lines as indicated by asterisk in lateral views. All scale bars = 1 cm.

Lobes are well denticulated.

Measurements: See Table 2 and Figs. 13, 14.

Discussion: The most striking difference between these specimens and those from the original locality (L-12682, Fig. 2B) described in Jenks et al. (2021) is the exceptional preservation of the present specimens' body chambers, several of which are undistorted and nearly complete. As is evident from the two scatter diagrams, the present specimens (Fig. 13) compare well morphologically with the specimens from the original locality (Fig. 14). See Jenks et al. (2021) for a thorough discussion of this taxon.

Occurrence: Float slabs of bivalve coquina at locality L-13032 (Figs. 2B, 3), located ~ 85 m west of the original Griesbachian ammonoid and nautiloid site.

***Wordieoceras mullenae* Jenks et al., 2021**
Figure 12Z-G'

p 1935 *Vishnuites decipiens* var. *discoidea*, Spath, p. 44, pl. XII, fig. 1; pl. XIII, fig. 4. Not pl. X, fig. 5.
2021 *Wordieoceras mullenae* Jenks et al., p. 13, figs. 8A-M.

Material: Three measured specimens; one (P-97312) consists of a partial phragmocone, the second (P-97313) consists of a nearly complete phragmocone and about 60% of the body chamber, while the third (P-97314) consists only of a partially complete phragmocone.

Description: (Largely taken from Jenks et al., 2021). Present specimens fairly small (~30 to 45 mm D) and fairly involute, compressed shell with gently convex flanks that converge to narrowly rounded venter. Ventral shoulders indistinct. Maximum whorl width occurs at 40 to 45% of whorl height. Flank contour broadly convex from top of umbilical shoulder to point of maximum whorl width, then converges more rapidly to venter, forming a high-whorled, sub-trigonal whorl section. Fairly narrow umbilicus (U/D avg, 0.24) with low, moderately steep wall and shoulders ranging from barely perceptible to broadly rounded. No obvious ornamentation on present specimens. Suture line with relatively low, broadly rounded saddles, fairly

wide, well denticulated first lateral lobe, finely denticulated 2nd lateral lobe and short auxiliary series with weak indentations.

Measurements: See Table 2 and Fig. 15.

Discussion: *Wordieoceras mullenae* differs from *W. wordiei* by its significantly smaller umbilicus. The present specimens agree fairly well with those from the original locality (L-12682, Fig. 2B) as seen in the scatter diagram comparison (Fig. 15). See Jenks et al. (2021) for a thorough discussion of *W. mullenae*.

Occurrence: Float slabs of bivalve coquina at locality L-13032 (Figs. 2B, 3).

Family INCERTAE SEDIS
Genus et species indet.
Figure 11V-Y

Occurrence: Very rare. One fairly well preserved, but very small specimen (P-97303) from the float block designated as L-13553, found just above L-13555 and below L-13552 in the Crittenden Springs-north section.

Description: Very small (D=~12 mm), moderately involute, fairly compressed shell (W/D=0.26, W/H=0.61) with convex flanks that converge gently from point of maximum whorl width to a moderately wide, tabulate venter with tightly rounded shoulders. Whorl section ovate with maximum width at ~35% of whorl height. Lower flank converges fairly rapidly to the abruptly rounded umbilical shoulder. Umbilicus fairly narrow (U/D=0.25) with low, very steep wall. Ornamentation not well preserved on much of shell, but ribs appear to be distant and sinuous. At least one prosiradiate, bullae-type rib visible that arises rapidly just above umbilical shoulder, gains maximum strength at about 30% of whorl height and fades rapidly just above mid-flank. Faint growth lines appear to follow ribbing. Suture line not known.

Discussion: Specimen occurs in earliest Dienerian with *Gyronites rigidus* and bears some resemblance to this taxon, but differs mainly by its much more involute coiling, i.e., narrower umbilicus (U/D=0.25 as compared to an average U/D of 0.37 for 25 specimens). Also, the low but distinctively steep umbilical

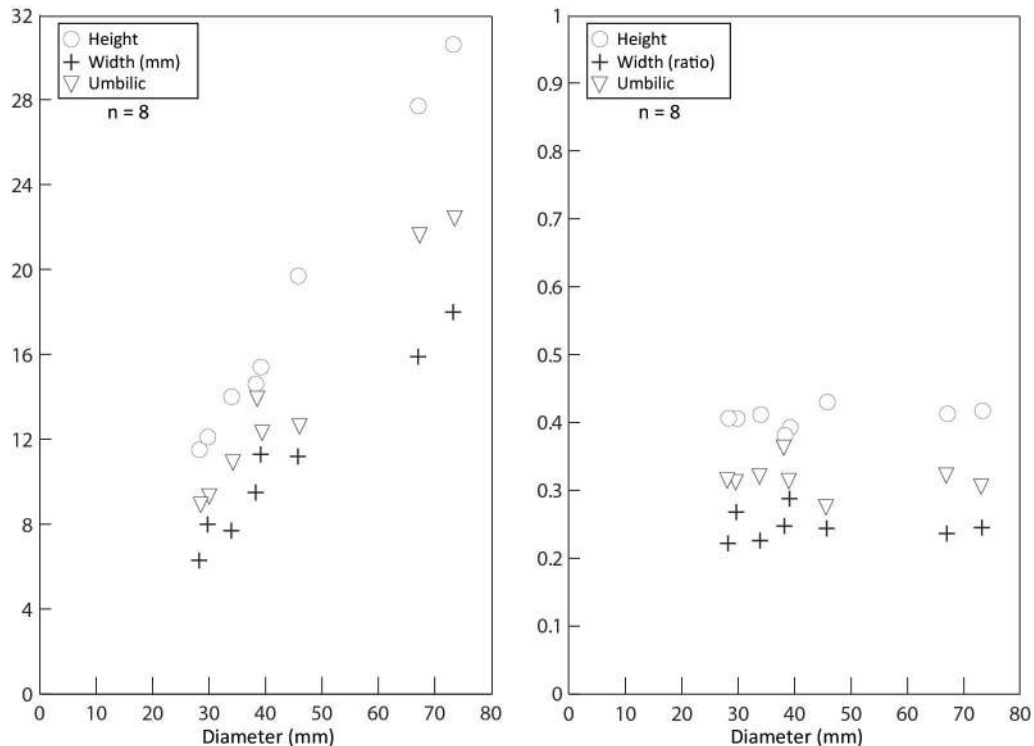


FIGURE 13. Scatter diagram comparison of H, W and U, and H/D, W/D and U/D for *Wordieoceras wordiei*.

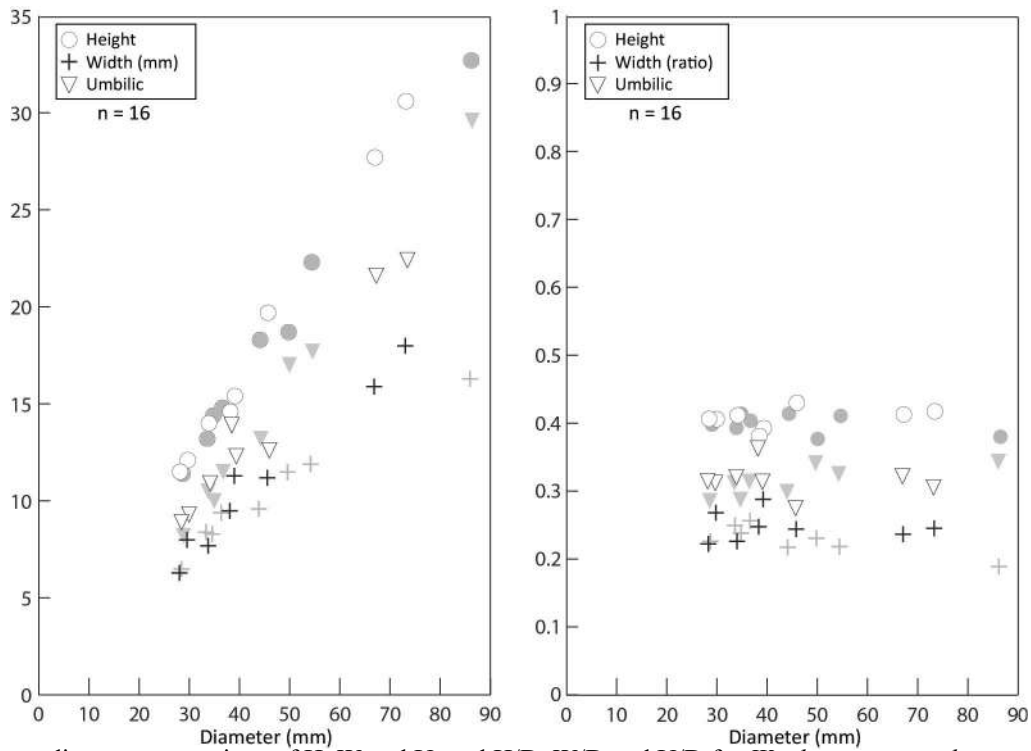


FIGURE 14. Scatter diagram comparison of H, W and U, and H/D, W/D and U/D for *Wordieoceras wordiei* specimens of present work from locality L-13032 (white circles and triangles, black crosses) vs. specimens (gray shaded figures) illustrated in Bulletin 86 (2021) from locality L-12682 (Figure 2).

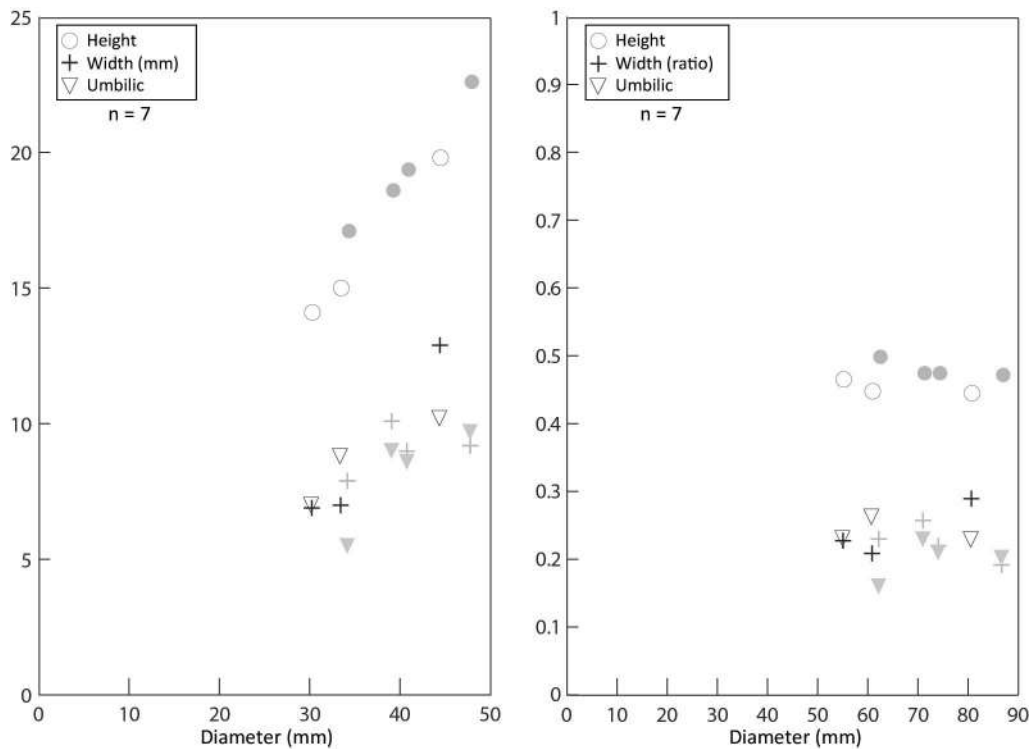


FIGURE 15. Scatter diagram comparison of H, W and U, and H/D, W/D and U/D for *Wordieoceras mullenae* specimens of present work from locality L-13032 (white circles and triangles, black crosses) vs. specimens (gray shaded figures) illustrated in Bulletin 86 (2021) from locality L-12682 (Figure 2).

wall contrasts with the lower flank of *G. rigidus* that meets the preceding whorl at an obtuse angle without a discernable wall. It is difficult to compare this extremely small specimen with the relatively much larger *G. rigidus* shells. It is possible that the specimen represents an immature shell, but the morphology of comparable sized *G. rigidus* shells is not known, at least from Crittenden Springs. In summary, additional material is needed to determine if this specimen represents a unique taxon.

Occurrence: The present specimen was found in float block L-13553 in the Crittenden Springs-north section (Figs. 2A, 3).

Order NAUTILIDA Agassiz, 1847
Superfamily TRIGONOCERATOIDEA Hyatt, 1884
Family GRYPOCERATIDAE Hyatt, 1900
Genus *Xiaohenautilus* Xu, 1988
Type species: *Xiaohenautilus sinensis* Xu, 1988
***Xiaohenautilus chatelaini* n. sp.**

Figure 16A-J

Type series: Two specimens, both of which are phragmocones: holotype, P-97317 (Fig. 16G-J); paratype, P-97316, (Fig. 16A-F).

Etymology: Named in honor of Edward Chatelain of Valdosta, Georgia.

Diagnosis: Moderately involute, fairly depressed *Xiaohenautilus* with subquadrate to elliptical whorl section, fairly narrow umbilicus and small umbilical perforation.

Description: Moderately involute, fairly depressed shell with subquadrate to elliptical whorl section, broadly rounded venter, rounded ventral shoulder and slightly convex flanks with maximum whorl width at mid-flank. Degree of whorl depression accentuated by fairly high expansion rate of whorl width. Umbilicus fairly narrow with moderately high, vertical wall and rounded shoulders. Umbilical perforation 2.0-3.3 mm. Embryonic shell and body chamber length unknown. Ornamentation consists of fine, sinuous growth lines with deep, V-shaped hyponomic sinus on venter. Siphuncle located near venter at one seventh of whorl height. Suture simple, typical of other *Xiaohenautilus* taxa, with shallow, wide ventral lobe.

Measurements: See Table 3. Note: Because the holotype (P-97317) is an incomplete whorl, its measurable portion (23.5 mm) is nearly the same as the paratype (P-97316; 21.9 mm). However, if the holotype's whorl was complete its diameter would be almost twice that of the paratype.

Discussion: *Xiaohenautilus chatelaini* n. sp. differs from other species of *Xiaohenautilus*, i.e., *X. sinensis* Xu (1988, p. 439), *X. huananensis* Xu (1988, p. 439), *X. abrekensis* Shigeta and Zakharov (2009, p. 53) and *X. mulleni* Jenks et al., (2012, p. 20) by its smaller umbilical perforation, more involute shell and more depressed whorls with a narrower umbilicus. *Xiaohenautilus chatelaini* n. sp. clearly differs from *X. mulleni* and *X. abrekensis* by its significantly higher W/H ratio, i.e., 1.08 vs 0.93 and 0.85, respectively. The difference between *X. mulleni* and *X. chatelaini* is exemplified by the former's compressed, nearly parallel flanks (see Fig. 16K-S) vs. the fairly rapidly expanding whorl width of the latter.

Occurrence: Present specimens found in bed L-13559 in the Crittenden Springs-north section (Figs. 2A, 3)

***Xiaohenautilus mulleni* Jenks et al., 2021**
Figure 16K-S

2021 *Xiaohenautilus mulleni* Jenks et al., p. 20, figs. 111-D'

Material: One float specimen (P-97315; Fig. 16K-O). Note: The holotype of *X. mulleni* Jenks et al. (NMMNH P-81693) is shown for comparative purposes (Fig. 16P-S).

Description: (Largely taken from Jenks et al., 2021). At early growth stage, moderately evolute, fairly compressed nautiloid with subquadrate whorl section, broadly rounded venter, rounded ventral shoulders and slightly convex flanks

with maximum whorl width just above umbilical shoulder. With increasing size, whorl section transitions to quadrate with broad subtabulate venter, abruptly rounded shoulders and nearly parallel flanks. Umbilicus fairly narrow with moderately high, vertical wall, rounded shoulders and fairly small (2-4 mm) umbilical perforation. Ornamentation consists of fine, sinuous growth lines with deep, V-shaped hyponomic sinus on venter. Siphuncle located near venter at one fifth of whorl height. Simple suture with shallow, wide ventral lobe.

Measurements: See Table 3.

Discussion: *Xiaohenautilus mulleni* was erected for five float specimens of late Griesbachian age from a narrow interval (~2.5 m, locality NMMNH L-12683) located ~ 11 m stratigraphically above the late Griesbachian ammonoid bed in the Dinwoody Formation at Crittenden Springs, Nevada (see Jenks et al., 2021). The early Dienerian-age present specimen, although badly weathered, fits quite well within the morphological parameters of *X. mulleni* and is therefore assigned to this taxon.

Occurrence: Present specimen found as float about 2 m east of locality L-13554 in the Crittenden Springs-north section, about 1.9 km north of Long Canyon (Figs. 2A, 3).

CONCLUSIONS

1. Continued field work in the Dinwoody Formation in the Crittenden Springs-north area (Nevada, USA) has resulted in the discovery of an early Dienerian ammonoid and nautiloid assemblage. This discovery represents the first report of early Dienerian cephalopods in eastern Panthalassa.

2. The early Dienerian ammonoid assemblage includes the genus *Gyronites*, heretofore known only from the Tethys and South Primorye.

3. The early Dienerian ammonoid assemblage correlates broadly with the three-fold subdivision of the early Dienerian of the NIM, with the exception of the middle ammonoid UAZ, whose eponymous taxon, i.e., *Gy. plicosus*, has not yet been found at Crittenden Springs.

4. Ongoing field work in the southern end of the outcrop area has led to a newly discovered occurrence of the late Griesbachian ammonoids *Wordieoceras wordiei* and *W. mullenae* ~85 m west of the original late Griesbachian ammonoid site.

5. One new nautiloid taxon, i.e., *Xiaohenautilus chatelaini* n. sp., is described from the *Gy. frequens* beds (L-13559) in the Crittenden Springs-north section..

6. The FO of the basal Dienerian marker conodont *Sweetospathodus kummeli* occurs ~30 m above the FO of the ammonoid *Gyronites*. This stratigraphic occurrence contrasts with the NIM and Arctic Canada localities where the conodont's FO is located slightly below the FO of basal Dienerian ammonoids. Thus, until more data becomes available, the utility of *S. kummeli* as an index conodont is questionable.

ACKNOWLEDGMENTS

J.F. Jenks acknowledges the patience and kind support of Ruby Jenks throughout this project. All field work was conducted on US public land (Bureau of Land Management) under the auspices of Paleontological Resources Use Permit number N-97816. We are grateful to BLM personnel in the Elko and Wells Field Offices for their cooperation. We thank reviewers Spencer Lucas, Romain Jattiot and Claude Monnet for their many helpful suggestions that significantly improved the manuscript. We are grateful to Rachael Paull and Chris and Donna Mullen for sharing their past research in the study area. Gilles Escarguel, Nicolas Olivier and Emmanuel Fara are thanked for their help in the field on May 25, 2023. Thanks are extended to Gento Shinohara, Shuhei Nomura and Takahiko Kutsuna for their efforts in the proper maintenance of the micro-CT scanner and software in the National Museum of Nature and Science Research Wing (NMNS, Tsukuba). This research was

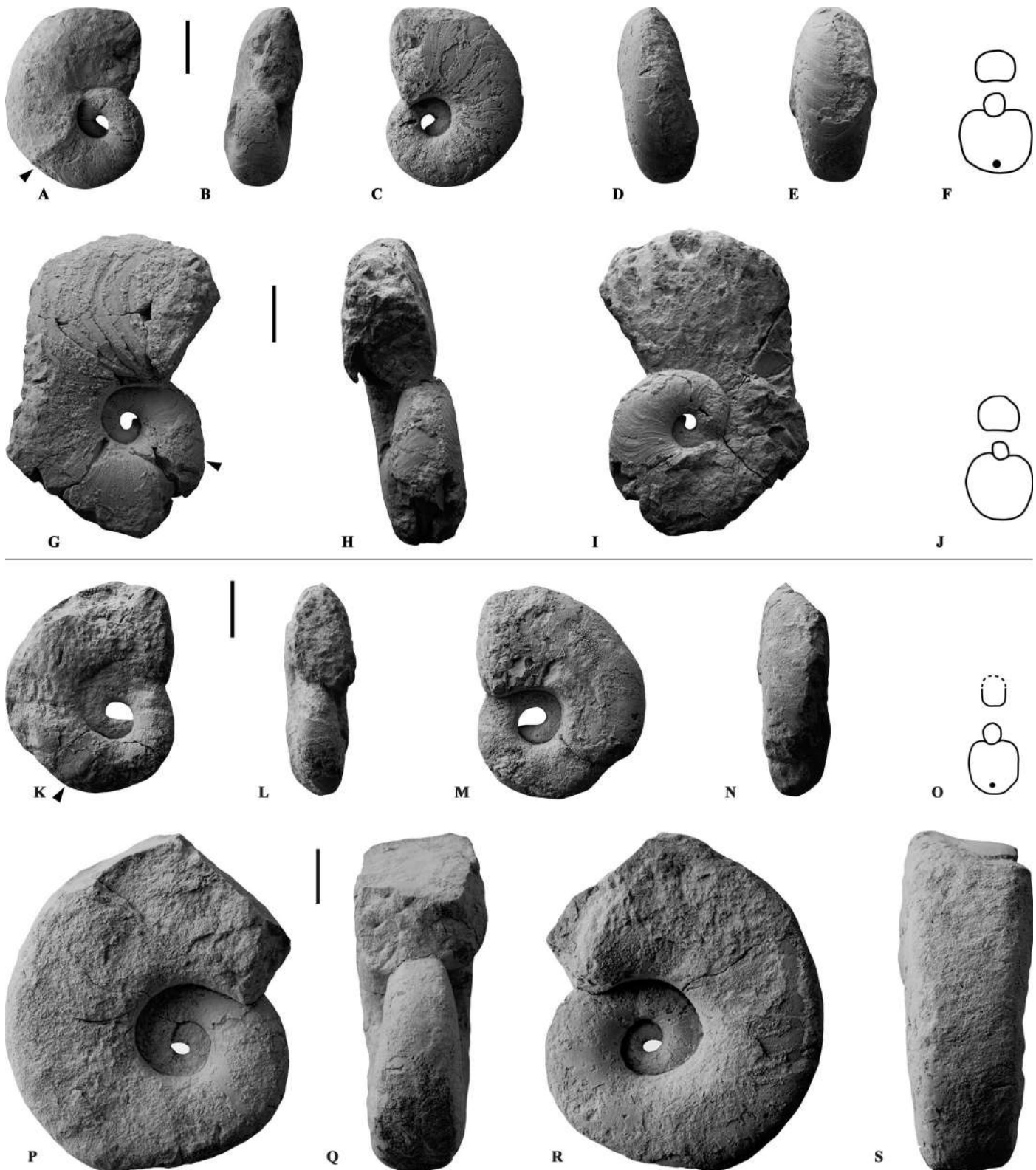


FIGURE 16. A-J, *Xiaohenautilus chatelaini* n. sp., in A-F, P-97316, L-13559, holotype, in A, left lateral, B, apertural, C, right lateral, D, ventral (1), and E, ventral (2) views, F, whorl cross section. G-J, P-97317, L-13559, paratype, in G, left lateral, H, apertural, and I, right lateral views, J, whorl cross section. K-S, *Xiaohenautilus mulleni* Jenks et al., in K-O, P-97315, float, near L-13554, in K, left lateral, L, apertural, M, right lateral, and N, ventral views, O, whorl cross section. P-S, P-81693, from L-12683, holotype, late Griesbachian (included for comparative purposes from NMMNH&S Bulletin 86), in P, left lateral, Q, apertural, R, right lateral and S, ventral views. All whorl cross sections from CT scan images, as indicated by position of black arrows in lateral views. All scale bars = 1 cm.

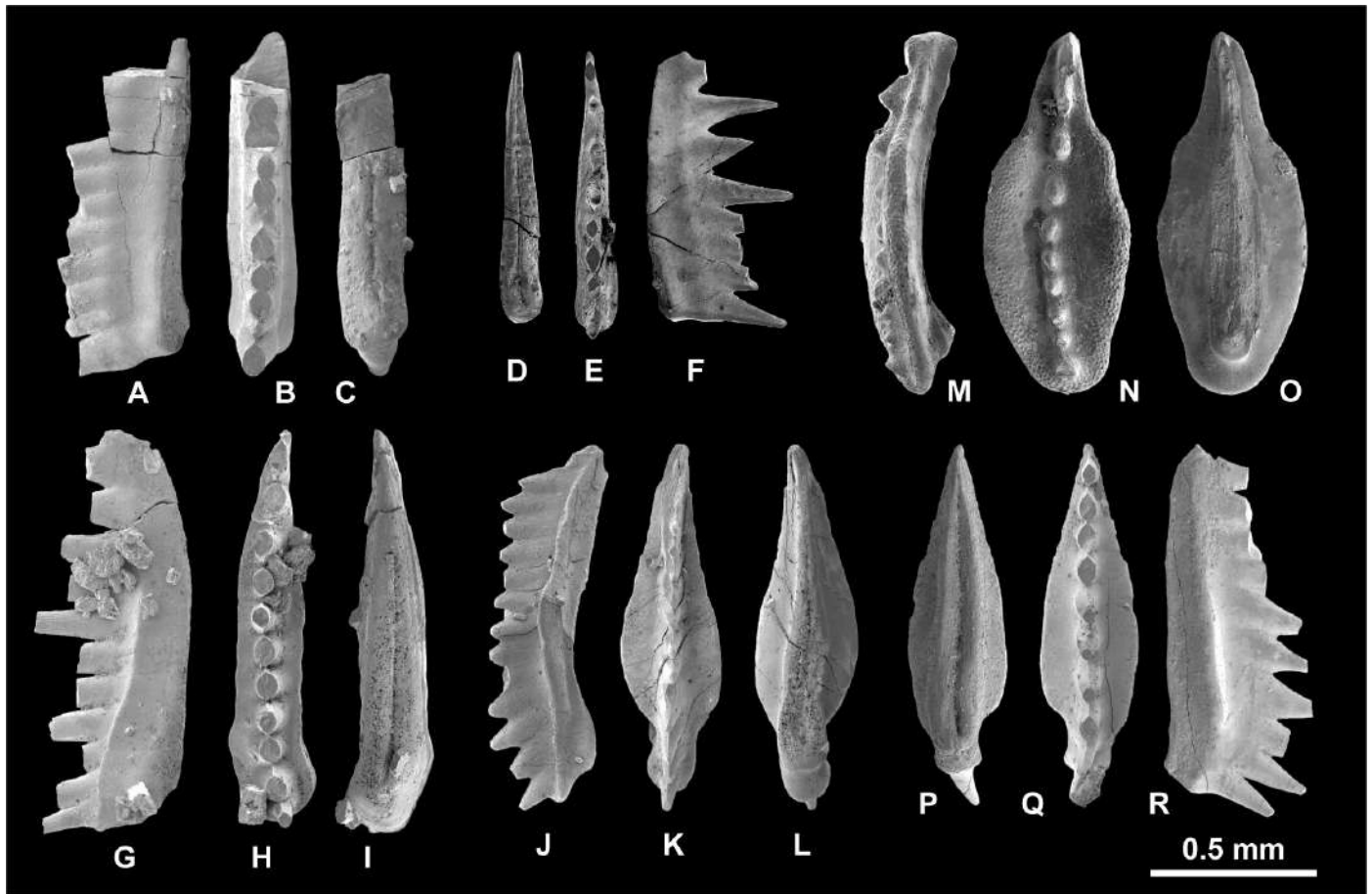


FIGURE 17. **A-I**, *Sweetospathodus kummeli* (Sweet), in **A-C**, P-97318 from locality L-13552, in **A**, lateral, **B**, upper and **C**, lower views. **D-F**, P-97319 from locality L-13553, in **D**, lower, **E**, upper and **F**, lateral views. **G-I**, P-97320, from L-13559, in **G**, lateral, **H**, upper and **I**, lower views. **J-L**, *Scythogondolella* sp., P-97321, from locality L-13559, in **J**, lateral, **K**, upper and **L**, lower views. **M-O**, *Clarkina nassichuki* (Orchard in Orchard and Krystyn), P-97322, from locality L-13032, in **M**, lateral, **N**, upper and **O**, lower views. **P-R**, *Neoclarkina discreta* (Orchard and Krystyn), P-97323, from L-13557, in **P**, lower, **Q**, upper and **R**, lateral views.

TABLE 2. Measurements, Late Griesbachian ammonoids from locality L-13032, Crittenden Springs.

LATE GRIESBACHIAN AMMONOIDS FROM LOCALITY L-13032, CRITTENDEN SPRINGS (measurements by hand unless otherwise indicated by asterisk)CT scan									
NMMNH P-	Taxon	D _{mm}	W	H	U	W/D	H/D	U/D	W/H
97304*	<i>Wordieoceras wordiei</i>	45.8	11.2	19.7	12.6	0.25	0.43	0.28	0.57
97305	<i>Wordieoceras wordiei</i>	39.2	11.3	15.4	12.3	0.29	0.39	0.31	0.73
97306	<i>Wordieoceras wordiei</i>	34.0	7.7	14.0	10.9	0.23	0.41	0.32	0.55
97307	<i>Wordieoceras wordiei</i>	29.8	8.0	12.1	9.3	0.27	0.41	0.31	0.66
97308	<i>Wordieoceras wordiei</i>	38.3	9.5	14.6	13.9	0.25	0.38	0.36	0.65
97309	<i>Wordieoceras wordiei</i>	28.3	6.3	11.5	8.9	0.22	0.41	0.31	0.55
97310	<i>Wordieoceras wordiei</i>	67.1	15.9	27.7	21.6	0.24	0.41	0.32	0.57
97311*	<i>Wordieoceras wordiei</i>	73.3	18.0	30.6	22.4	0.25	0.42	0.30	0.59
97312	<i>Wordieoceras mullenae</i>	33.5	7.0	15.0	8.8	0.21	0.45	0.26	0.47
97313*	<i>Wordieoceras mullenae</i>	30.3	6.9	14.1	7.0	0.23	0.47	0.23	0.49
97314	<i>Wordieoceras mullenae</i>	44.5	12.9	19.8	10.2	0.29	0.44	0.23	0.65

* indicates measurements by CT scan.

TABLE 3. Measurements, Early Dienerian nautiloids from Crittenden Springs- north area.

EARLY DIENERIAN NAUTILOIDS FROM CRITTENDEN SPRINGS- NORTH AREA											
(all measurements from CT scan images)											
NMMNH P-	Taxon	NMMNH L-	D _{mm}	W	H	U	W/D	H/D	U/D	W/H	UP
97315	<i>Xiaohenautilus mulleni</i>	13554	24.5	10.0	11.1	7.0	0.41	0.45	0.29	0.90	3.14-5.43
97316	<i>X. chatelaini</i> n. sp.	13559	21.9	12.7	11.2	5.1	0.58	0.51	0.23	1.14	2.02-3.33
97317	<i>X. chatelaini</i> n. sp.	13559	23.5	12.5	12.3	4.5	0.53	0.52	0.19	1.02	2.04-3.26

financially supported by the 2019 annual research grant of the Fukuda Geological Institute (Fukuda Grant-in-Aid), the 2020 Nakatsuji Foresight Foundation Research Grant, and Grant-in-Aids for Young Research (KAKENHI) from the Japan Society for the promotion of Science (21K14036) to T. Maekawa.

AUTHOR CONTRIBUTIONS

FFJ: Wrote most of the manuscript. Found fossil localities and collected fossils. Prepared most of the ammonoids and aided in their identification. Created all ammonoid and nautiloid plates.

TM: Found fossil localities. Wrote portions of the manuscript that deal with conodonts. Sampled all localities for conodonts, processed all samples and identified conodonts. Created Figure 3 (biostratigraphic log), photographed conodonts and created conodont plate.

YS: Wrote portion of manuscript that deals with nautiloid systematic paleontology. Prepared nautiloid specimens. Photographed all specimens. Conducted CT scans on all specimens and used images to generate drawings of whorl cross sections. Made plaster casts of nearly all specimens. Identified problematic ammonoid taxa.

DW: Identified ammonoid specimens found during first year of present study. Confirmed identity of all problematic ammonoid taxa.

AB: Performed statistical analysis (scatter diagrams, box plots) on most ammonoid taxa. Corroborated identity of problematic ammonoid taxa. Constructed Figures 1 and 4.

KGB: Found fossil localities. Collected ammonoids from several localities and collected specimens representing the new nautiloid taxon.

DAS: Collected ammonoid specimens from several localities.

NK: Found ammonoid localities and collected ammonoid specimens from several localities.

All authors read first draft of manuscript and provided valuable suggestions for improvement.

REFERENCES

- Agassiz, L., 1847, Lettres sur quelques points d'organisation des animaux rayonnés: Comptes Rendus de l'Académie des Sciences, v. 25, p. 677-682.
- Arthaber, G.V., 1911, Die Trias von Albanien: Beiträge zur Paläontologie und Geologie Österreich-Ungarns und des Orients, v. 24, p. 169-276.
- Blackwelder, E., 1918, New geological formations in western Wyoming: Washington Academy Science Journal, v. 8, p. 417-426.
- Bjerager, M., Siedler, L., Stemmerik, L. and Finn, S.K., 2006, Ammonoid stratigraphy and sedimentary evolution across the Permian-Triassic boundary in East Greenland: Geological Magazine, v. 143, p. 635-656.
- Brayard, A., Bucher, H., Escarguel, G., Fluteau, F., Bourquin, S. and Galfetti, T., 2006, The Early Triassic ammonoid recovery: Paleoclimatic significance of diversity gradients: Palaeogeography, Palaeoclimatology, Palaeoecology 239, p. 374-395.
- Brayard, A., Brühwiler, T., Galfetti, T., Goudemand, N., Guodun, K., Escarguel, G. and Jenks, J.F., 2007, *Proharpoceras* Chao: A new ammonoid lineage surviving the end-Permian mass extinction: Lethaia, v. 40, p. 175-181.
- Brayard, A. and Bucher, H., 2008, Smithian (Early Triassic) ammonoid faunas from northwestern Guangxi (South China): taxonomy and biochronology: Fossils and Strata, v. 55, 184 p.
- Brayard, A. and Bucher, H., 2015, Permian-Triassic extinctions and rediversifications; in Klug, C., et al., eds., Ammonoid Paleobiology: From Macroevolution to Paleogeography: Topics in Geobiology, 44: New York, Springer, p. 465-473.
- Brayard, A., Escarguel, G., Bucher, H., Monnet, C., Brühwiler, T., Goudemand, N., Galfetti, T. and Guex, J., 2009, Good genes and good luck: Ammonoid diversity and the end-Permian mass extinction: Science, v. 325, p. 1118-1121.
- Brayard, A., Krumenacker, L.J., Botting, J.P., Jenks, J.F., Bylund, K.G., Fara, E., Vennin, E., Olivier, N., Goudemand, N., Saucède, T., Charbonnier, S., Romano, C., Doguzhaeva, L., Thuy, B., Hautmann, M., Stephen, D.A., Thomazo, C., and Escarguel, G., 2017, Unexpected Early Triassic marine ecosystem and the rise of the Modern evolutionary fauna: Science Advances, v. 3, 11 p.
- Brayard, A., Jenks, J.F., Bylund, K.G. and the Paris Biota Team, 2019, Ammonoids and nautiloids from the earliest Spathian Paris Biota and other early Spathian localities in southeastern Idaho, USA: Geobios, v. 54, p. 13-36.
- Brosse, M., Baud, A., Bhat, G.M., Bucher, H., Leu, M., Vennemann, T. and Goudemand, N., 2017, Conodont-based Griesbachian biochronology of the Guryul Ravine section (basal Triassic, Kashmir, India): Geobios, v. 50, p. 359-387.
- Brühwiler, T., Brayard, A., Bucher, H. and Guodun, K., 2008, Griesbachian and Dienerian (Early Triassic) ammonoid faunas from Northwestern Guangxi and Southern Guizhou (South China): Palaeontology, v. 51, p. 1151-1180.
- Brühwiler, T., Ware, D., Bucher, H., Krystyn, L. and Goudemand, N., 2010, New Early Triassic ammonoid faunas from the Dienerian/Smithian boundary beds at the Induan/Olenekian GSSP candidate at Mud (Spiti, Northern India): Journal of Asian Earth Sciences, v. 39, p. 724-739.
- Brühwiler, T., Bucher, H. and Krystyn, L., 2012, Middle and late Smithian (Early Triassic) ammonoids from Spiti, India: Special Papers in Palaeontology, v. 88, p. 115-174.
- Caravaca, G., Brayard, A., Vennin, E., Guiraud, M., Le Pourhiet, L., Grosjean, A., Thomazo, C., Olivier, N., Jenks, J.F., Bylund, K.G. and Stephen, D.A., 2017, Controlling factors for differential subsidence in the Sonoma Foreland Basin (Early Triassic, western USA): Geological Magazine, v. 155, p. 1305-1329.
- Carr, T.R., 1981, Paleogeography, depositional history and conodont paleoecology of the Lower Triassic Thaynes Formation in the Cordilleran miogeosyncline [PhD thesis]: University of Wisconsin-Madison, 210 p.
- Carr, T.R. and Paull, R.K., 1983, Early Triassic stratigraphy and paleogeography of the Cordilleran miogeocline; in Dolly, E.D., Reynolds, M.W. and Spearing, D.R., eds., Mesozoic paleogeography of the west-central United States: Society of Economic Paleontologists and Mineralogists, Rocky Mountain

- Section, Rocky Mountain Paleogeography Symposium 2, 55 p.
- Chen, Z.Q. and Benton, J.J., 2012, The timing and pattern of biotic recovery following the end-Permian mass extinction: *Nature Geoscience*, v. 5, p. 375-383.
- Clark, D.L., 1957, Marine Triassic stratigraphy in eastern Great Basin: *American Association of Petroleum Geologists Bulletin*, v. 41, p. 2192-2222.
- Collinson, J.W. and Hasenmueller, W.A., 1978, Early Triassic paleogeography and biostratigraphy of the Cordilleran miogeosyncline; in Howell, D.G. and McDougall, K.A., eds., *Mesozoic paleogeography of the western United States: Society of Economic Paleontologists and Mineralogists, Pacific Section, Pacific Coast Paleogeography Symposium 2*, p. 175-187.
- Cuvier, G.L.C.F.D., 1797, An 6: *Tableau Élémentaire de l'Histoire Naturelle des Animaux* 14, Baudouin, Paris, 710 p.
- Dagys, A. and Weitschat, W., 1993, Correlation of the Boreal Triassic: *Mitteilungen aus dem Geologisch-Paläontologischen Institut der Universität Hamburg*, v. 75, p. 249-256.
- Dagys, A. and Ermakova, S., 1996, Induan (Triassic) ammonoids from north-eastern Asia: *Revue de Paléobiologie*, v. 15, p. 401-447.
- Dai, X., Song, H., Brayard, A. and Ware, D., 2019, A new Griesbachian-Dienerian (Induan, Early Triassic) ammonoid fauna from Gujiaio, South China: *Journal of Paleontology*, v. 93, p. 48-71.
- Dai, X., Davies, J.H.F.L., Yuan, Z., Brayard, A., Ovtcharova, M., Guanghui, X., Xiaokang, L., Smith, C.P.A., Schweitzer, C.E., Mingtao, L., Perrot, B.G., Jiang, S., Miao, L., Cao, Y., Yan, J., Bai, R., Wang, F., Guo, W., Song, H., Tian, L., Dal Corso, J., Liu, Y., Chu, D., and Song, H., 2023a, A Mesozoic fossil Lagerstätte from 250.8 million years ago shows a modern-type marine ecosystem: *Science*, v. 379, p. 567-572.
- Dai, X., Brayard, A., Ware, D., Jiang, S., Li, M., Wang, F., Liu, X. & Song, H., 2023b, High-resolution Early Triassic ammonoid biostratigraphy of South Tibet, China and implications for global correlations: *Earth-Science Reviews*, <https://doi.org/10.1016/j.earscirev.2023.104384>.
- de Koninck, L.G., 1863, Description of some fossils from India, discovered by Dr. A. Fleming, of Edinburgh: *The Quarterly Journal of the Geological Society of London*, v. 19, 19 p.
- Diener, C., 1895, Triadische Cephalopodenfaunen der Ostsibirischen Küstenprovinz: *Mémoires du Comité Géologique St. Petersburg* 14, 59 p.
- Diener, C., 1897, Part I: the Cephalopoda of the Lower Trias: *Palaeontologia Indica*, Series 15, Himalayan Fossils 2, 181 p.
- Gardner, G.E., Jr., 2000, Color patterns, habitat, and sub-lethal events for Lower Triassic ammonoids from Crittenden Springs, Elko County, Nevada [M.S. thesis]: Athens, Ohio University, 420 p.
- Gardner, G.E., Jr. and Mapes, R.H., 2000, The relationships of color patterns and habitat for Lower Triassic ammonoid from Crittenden Springs, Elko County, Nevada: *Revue de Paléobiologie*, Genève, v. 8, p. 109-122.
- Griesbach, C.L., 1880, Palaeontological notes on the Lower Trias of the Himalayas: *Records of the Geological Survey of India* 13, p. 94-113.
- Guex, J., 1978, Le Trias inférieur des Salt Ranges (Pakistan): problèmes biochronologiques: *Ecologiae Geologia Helvetica*, v. 71, p. 105-141.
- Haggart, J.W., 1989, New and revised ammonites from the Upper Cretaceous Nanaimo Group of British Columbia and Washington State: *Geological Survey of Canada Bulletin*, v. 396, p. 181-221.
- Hallam, A., 1991, Why was there a delayed radiation after the end-Palaeozoic extinction?: *Historical Biology*, v. 5, p. 257-262.
- Han, C., Orchard, M.J., Wu, S., Zhao, L., Chen, Z.-Q., Golding, M.L., Jan, I.U., Lyu, Z. and Hashmi, S.I., 2022, Improved taxonomic definition based on the ontogenetic series of Griesbachian-Dienerian conodonts from the Early Triassic of northwestern Pakistan: *Global and Planetary Change*, v. 208: 103703.
- Hofmann, R., Hautmann, M. and Bucher, H., 2013, A new paleoecological look at the Dinwoody Formation (Lower Triassic, Western USA): Intrinsic versus extrinsic controls on ecosystem recovery after the End-Permian mass extinction: *Journal of Paleontology*, v. 87, p. 854-880.
- Hope, R.A. and Coates, R.R., 1976, Preliminary geologic map of Elko County, Nevada: U.S. Geological Survey Open-File Map 76-779, 1:100,000.
- Hose, R.K. and Repenning, C.A., 1959, Stratigraphy of Pennsylvanian, Permian, and Lower Triassic rocks of Confusion Range, west-central Utah: *American Association of Petroleum Geologists Bulletin*, v. 43, p. 2167-2196.
- Hu, S., Zhang, Q., Chen, Z.-Q., Zhou, C., Lü, T., Wen, W., Huang, J., and Benton, M.J., 2011, The Luoping biota: exceptional preservation and new evidence on the Triassic recovery from end-Permian mass extinction: *Proceedings of the Royal Society B: Biological Sciences*, v. 278, p. 2274-2282.
- Hyatt, A., 1884, Genera of fossil cephalopods: *Proceedings of the Boston Society of Natural History*, v. 22, p. 253-338.
- Hyatt, A., 1900, Cephalopoda; in K.A. Zittel, ed., *Textbook of palaeontology*; C.R. Eastman, p. 502-592.
- Jattiot, R., Bucher, H., Brayard, A., Brosse, M., Jenks, J.F. and Bylund, K., 2017, Smithian ammonoid faunas from northeastern Nevada: implications for Early Triassic biostratigraphy and correlations within the western USA basin: *Palaeontographica*, Abt. A, v. 309, 89 p.
- Jenks, J.F., 2007, Smithian (Early Triassic) ammonoid biostratigraphy at Crittenden Springs, Elko County, Nevada and a new ammonoid from the *Meekoceras gracilitatis* Zone: *New Mexico Museum of Natural History and Science, Bulletin* 40, p. 81-90.
- Jenks, J.F., Brayard, A., Brühwiler, T. and Bucher, H., 2010, New Smithian (Early Triassic) ammonoids from Crittenden Springs, Elko County, Nevada: Implications for taxonomy, biostratigraphy and biogeography: *New Mexico Museum of Natural History and Science, Bulletin* 48, 41 p.
- Jenks, J.F., Monnet, C., Balini, M., Brayard, A. and Meier, M., 2015, Biostratigraphy of Triassic ammonoids; in Klug, C., et al., eds., *Ammonoid Paleobiology: From Macroevolution to Paleogeography: Topics in Geobiology*, v. 44, New York, Springer, p. 329-388.
- Jenks, J.F. and Brayard, A., 2018, Smithian (Early Triassic) ammonoids from Crittenden Springs, Elko County, Nevada: taxonomy biostratigraphy and biogeography: *New Mexico Museum of Natural History and Science, Bulletin* 78, 175 p.
- Jenks, J.F., Maekawa, T., Ware, D., Shigeta, Y., Brayard, A. and Bylund, K.G., 2021, Late Griesbachian (Early Triassic) ammonoids and nautiloids from the Dinwoody Formation at Crittenden Springs, Elko County, Nevada: *New Mexico Museum of Natural History & Science, Bulletin* 86, 23 p.
- Korn, D., Leda, L., Heuer, F., Salimi, H.M., Farshid, E., Akbari, A., Schobben, M., Ghaderi, A., Struck, U., Gliwa, J., Ware, D. and Hairapetian, V., 2021, Baghuk Mountain (Central Iran): high-resolution stratigraphy of a continuous Central Tethyan Permian-Triassic boundary section: *Fossil Record*, v. 24, p. 171-192.
- von Krafft, A. and Diener, C., 1909, Lower Triassic Cephalopoda from Spiti, Malla, Johar, and Byans: *Palaeontologia Indica*, v. 6, 186 p.
- Krystyn, L., Richoz, S., Baud, A., Twichett, R.J., 2003, A unique Permian-Triassic boundary section from the Neotethyan Hawasina Basin, Central Oman Mountains: *Palaeogeography, Palaeoclimatology, Palaeoecology*, v. 191, p. 329-344.
- Krystyn, L., Balini, M., and Nicora, A., 2004, Lower and Middle Triassic stage and substage boundaries in Spiti: *Albertiana*, v. 3, p. 40-53.
- Krystyn, L., Bhargava, O.N. and Richoz, S., 2007a, A candidate GSSP for the base of the Olenekian Stage: Mud at Pin Valley; district Lahul and Spiti, Himachal Pradesh (Western Himalaya), India: *Albertiana*, v. 35, p. 5-29.
- Krystyn, L., Richoz, S., and Bhargava, O.N., 2007b, The Induan-Olenekian Boundary (IOB) in Mud-An update of the candidate GSSP section M04: *Albertiana*, v. 36, p. 33-45.

- Kummel, B., 1954, Triassic Stratigraphy of southeastern Idaho and adjacent areas: U.S. Geological Survey, Professional Paper 254-H, p.165-194.
- Kummel, B. and Steele, G., 1962, Ammonites from the *Meekoceras gracilitatis* Zone at Crittenden Springs, Elko County, Nevada: *Journal of Paleontology*, v. 36, p. 638-703.
- Lucas, S.G., Krainer, K. and Milner, A.R.C., 2007, The type section and age of the Timpoweap Member and stratigraphic nomenclature of the Triassic Moenkopi Group in southwestern Utah: *New Mexico Museum of Natural History and Science, Bulletin* 40, p. 109-117.
- Maekawa, T. and Jenks, J.F., 2021, Smithian (Olenekian, Early Triassic) conodonts from ammonoid-bearing limestone blocks at Crittenden Springs, Elko County, Nevada, USA: *Paleontological Research*, v. 25 (3), p. 201-245.
- Mapes, R.H. and Sneek, D.A., 1987, The oldest ammonoid color patterns: Description, comparison with *Nautilus*, and implications: *Paleontology*, v. 30, p. 299-309.
- Mapes, R. H. and Davis, R.A., 1996, Color patterns in ammonoids; *in* Landman, H.H., Tanabe, K. and Davis, R.A., eds, *Ammonoid Paleobiology*: Plenum, New York, NY, p. 104-127.
- Mu, L. Zakharov, Y.D., Li, W., Shen, S, 2007, Early Induan (Early Triassic) cephalopods from the Daye Formation at Guiding, Guizhou Province, South China: *Journal of Paleontology*, v. 81, p.858-872.
- Mullen, D.M., 1985a, Structure and stratigraphy of Triassic rocks in the Long Canyon area, northeastern Elko County, Nevada [M.S. thesis]: University of Wisconsin-Milwaukee.
- Mullen, C.E., 1985b, Structure and Stratigraphy of Triassic Rocks in the Immigrant Canyon area, northeast Elko County, Nevada [M.S. thesis]: University of Wisconsin-Milwaukee.
- Muller, S.W. and Ferguson, H.G., 1939, Mesozoic stratigraphy of the Hawthorne and Tonopah Quadrangles, Nevada: *Geological Society America Bulletin*, v. 50, p. 1573-1624.
- Newell, N.D. and Kummel, B., 1942, Lower Eo-Triassic stratigraphy, western Wyoming and southeast Idaho: *Geological Society of America Bulletin*, v. 53, p. 937-996.
- Noetling, F., 1905, Die asiatische Trias; *in* Frech, F., ed., *Lethaea Geognostica, Das Mesozoicum*, Verlag der E. Schweizerbart'schen Verlagsbuchhandlung (E. Nägele), Stuttgart, Germany, v. 1, p. 107-221.
- Orchard, M.J., 2007, Conodont diversity and evolution through the latest Permian and Early Triassic upheavals: *Palaeogeography, Palaeoclimatology, Palaeoecology*, v. 252, p. 93-117.
- Orchard, M.J., 2008, Lower Triassic conodonts from the Canadian Arctic, their intercalibration with ammonoid-based stages and a comparison with other North American Olenekian faunas: *Polar Research*, v. 27, p. 393-412.
- Paull, R.K., 1980, Conodont biostratigraphy of the Lower Triassic Dinwoody Formation in northwestern Utah, northeastern Nevada and southeastern Idaho [PhD thesis]: University of Wisconsin-Madison.
- Paull, R.A. and Paull, R.K., 1994, Tectonic control along the southern and western margins of the Lower Triassic Dinwoody depositional basin within the Cordilleran miogeocline: *GSA Abstracts with Programs*, v. 26, n. 6, p. 58.
- Poole, F.G. and Wardlaw, B.R., 1978, Candelaria (Triassic) and Diablo (Permian) Formations in southern Toquima Range, Central Nevada, *in* Howell, D.G. and McDougall, K.A., eds., *Mesozoic Paleogeography of the Western United States: Pacific Coast Paleogeography Symposium 2*, p. 271-276.
- Raup, D.M., 1979, Size of the Permo-Triassic bottleneck and its evolutionary implications: *Science*, v. 206, p. 217-218.
- Shigeta, Y. and Zakharov, Y.D., 2009, Systematic Paleontology, Cephalopods; *in* Shigeta, Y., Zakharov, Y.D., Maeda, H. and Popov, A.M., eds., *The Lower Triassic system in the Abrek Bay area, South Primorye, Russia: National Museum of Nature and Science Monographs No. 38.*, p. 44-140.
- Silberling, N.J., 1973, Geologic events during Permian-Triassic time along the Pacific margin of the United States; *in* Logan, A. and Hills, L.V., eds., *The Permian and Triassic Systems and their mutual boundary: Canadian Society Petroleum Geologists, Mem.* 2, p. 345-362.
- Smith, C.P.A., Laville, T., Fara, E., Escarguel, G., Oliver, N., Vennin, E., Goudemand, N., Bylund, K.G., Jenks, J.F., Stephen, D.A., Hautmann, M., Charbonner, S., Krumenacker, L.J. and Brayard, A., 2021, Exceptional fossil assemblages confirm the existence of complex Early Triassic ecosystems during the early Spathian: *Scientific Reports*, v. 11, 19657.
- Song, H., Wignall, P.B., Chen, Z., Tong, J., Bond, D.P., Lai, X., Zhao, X., Jiang, H., Yan, C. and Niu, Z., 2011, Recovery tempo and pattern of marine ecosystems after the end-Permian mass extinction: *Geology*, v. 39, p. 739-742.
- Song, H., Wignall, P.B., Tong, J. and Yin, H., 2013, Two pulses of extinction during the Permian-Triassic crisis: *Nature Geoscience*, v. 6, p. 52-56.
- Spath, L.F., 1930, The Eotriassic invertebrate fauna of East Greenland: *Meddelelser om Grønland*, v. 83, 87 p.
- Spath, L.F., 1934, Catalogue of the Fossil Cephalopoda of the British Museum (Natural History), Part IV: The Ammonoidea of the Trias, 521 p., 18 pl.
- Spath, L.F., 1935, Additions to the Eo-Triassic invertebrate fauna of East Greenland: *Meddelelser om Grønland*, v. 98, 115 p.
- Stanley, S.M., 2016, Estimates of the magnitudes of major marine mass extinctions in earth history: *Proceedings of the National Academy of Sciences*, v. 113, no. 42, p. E6325-E6334, doi: 10.1073/pnas.1613094113.
- Sweet, W.C., 1970, Uppermost Permian and Lower Triassic conodonts of the Salt Range and Trans-Indus Ranges, West Pakistan: *The University Press of Kansas, USA*, p. 207-275.
- Sweet, W.C., Mosher, L.C., Clark, D.L., Collinson, J.W. and Hasenmueller, W.H., 1971, Conodont biostratigraphy of the Triassic; *in* Sweet, W.C. and Bergstrom, S.M., eds., *Symposium on Conodont biostratigraphy: Geological Society of America Memoir 127*, p. 441-465.
- Tong, J., Zhang, S., Zuo, J. and Xiong, X., 2007, Events during Early Triassic recovery from the end-Permian extinction: *Global and Planetary Change*, v. 55, p. 66-80.
- Tozer, E.T., 1965, Lower Triassic stages and ammonoid zones of Arctic Canada: *Geological Survey of Canada, Paper 65-12*, 14 p.
- Tozer, E.T., 1967, A standard for Triassic time: *Geological Survey of Canada, Bulletin 156*, 103 p.
- Tozer, E.T., 1971, Triassic Time and Ammonoids: Problems and Proposals: *Canadian Journal of Earth Sciences*, v. 8, p.989-1031.
- Tozer, E.T., 1981, Triassic Ammonoidea: classification, evolution and relationship with Permian and Jurassic forms; *in* House, M.R. and Senior, J.R., eds., *The Ammonoidea: The Systematics Association*, London p. 65-100.
- Tozer, E.T., 1984, The Trias and its ammonoids: the evolution of a timescale: *Geological Survey of Canada, Miscellaneous Report 35*, 171 p.
- Tozer, E.T., 1994, Canadian Triassic ammonoid faunas: *Geological Survey of Canada, Bulletin 467*, 663 p.
- Waagen, W., 1895, *Salt Ranges Fossils*, v. 2: Fossils from the ceratite formation, part 1, Pisces-Ammonoidea: *Palaeontologia Indica*, Series 13, 2: 323 p.
- Wang, Y. and He, G., 1976, Triassic ammonoids from the Mount Jolmo Lungma region; *in* A report of the scientific expedition in the Mount Jolmo Lungma region (1966-1968): *Paleontology*, v. 3, p. 223-502.
- Wang, Y., 1984, Earliest Triassic ammonoid faunas from Jiangsu and Zhejiang and their bearing on the definition of Permo-Triassic boundary: *Acta Palaeontologica Sinica*, v. 23, p. 257-269.
- Wardlaw, B.R., Collinson, J.W. and Ketner, K.B., 1979, Regional relations of Middle Permian rocks in Idaho, Nevada and Utah; *in* Newman, G.W. and Goode, H.D., eds., *Basin and Range Symposium: Rocky Mountain Association of Geologists and Utah*

- Geological Association, Denver, p. 277-283.
- Ware, D., Jenks, J.F., Hautmann, M. and Bucher, H., 2011, Dienerian (Early Triassic) ammonoids from the Candelaria Hills (Nevada, USA) and their significance for palaeobiogeography and palaeoceanography: *Swiss Journal of Geoscience*, v. 104, p. 161-181.
- Ware, D., Bucher, H., Brayard, A., Schneebeli-Hermann, E. and Brühwiler, T., 2015, High-resolution biochronology and diversity dynamics of the Early Triassic ammonoid recovery: the Dienerian faunas of the Northern Indian Margin: *Palaeogeography, Palaeoclimatology, Palaeoecology*, v. 440, p. 363-373.
- Ware, D., Bucher, H., Brühwiler, T., Schneebeli-Hermann, E., Hochuli, P.A., Roohi, G., Ur-Rehman, K. and Yaseen, A., 2018a, Griesbachian and Dienerian (Early Triassic) ammonoids from the Salt Range, Pakistan: *Fossils and Strata*, p. 11-175.
- Ware, D. and Bucher, H., 2018a, *Systematic Paleontology*; in Ware, D., Bucher, H., Brühwiler, T., Schneebeli-Hermann, E., Hochuli, P.A., Roohi, G., Ur-Rehman, K. and Yaseen, A., Griesbachian and Dienerian (Early Triassic) ammonoids from the Salt Range, Pakistan: *Fossils and Strata*, p. 11-175.
- Ware, D. Bucher, H., Brühwiler, T. and Krystyn, L., 2018b, Dienerian (Early Triassic) ammonoids from Spiti, Himachal Pradesh, India: *Fossils and Strata*, p. 179-241.
- Ware, D. and Bucher, H., 2018b, *Systematic Paleontology*, in Ware, D., Bucher, H., Brühwiler, T. and Krystyn, L., Dienerian (Early Triassic) ammonoids from Spiti, Himachal Pradesh, India: *Fossils and Strata*, p. 179-241.
- Waterhouse, J.B., 1996, The early and middle Triassic ammonoid succession of the Himalayas in western and central Nepal, part 2, systematic studies of the early Middle Scythian: *Palaeontographica, Abteilung A*, v. 241, p. 27-100.
- Weitschat, W. and Dagys, A., 1989, Triassic biostratigraphy of Svalbard and comparison with NE-Siberia: *Mitteilungen aus dem Geologisch-Paläontologischen Institut der Universität Hamburg*, v. 68, p. 179-213.
- Xu, G.H., 1988, Early Triassic cephalopods from Lichuan, Western Hubei: *Acta Palaeontologia Sinica*, v. 27, p. 437-456. (In Chinese with English summary).
- Zakharov, Y.D., 1968, Lower Triassic biostratigraphy and ammonoids of South Primorye: *Nauka, Moskva*, 175 p. (in Russian).
- Zakharov, Y. D. and Rybalka, S. V., 1987, A standard for the Permian-Triassic in the Tethys; in *Problems of the Permian and Triassic biostratigraphy of east U.S.S.R.*, Vladivostok, p. 6-48.
- Zakharov, Y.D. and Mu, L., 2007, *Systematic Paleontology*; in Mu L., Zakharov Y.D., Li W.-Z & Shen S.-Z., 2007, Early Induan (Early Triassic) cephalopods from the Daye Formation at Guiding, Guizhou Province, South China: *Journal of Paleontology*, v. 81, p. 860-872.
- Zhang, C., Bucher, H. and Shen, S-Z, 2017, Griesbachian and Dienerian (Early Triassic) ammonoids from Qubu in the Mt. Everest area, southern Tibet: *Paleoworld*, v. 26, p. 650-662.

APPENDIX

Presented below are the World Geodetic System (WGS) and US Public Land Survey coordinates for the nine localities discussed in this work.

NMMNH Locality number	WGS coordinates	US Public Land Survey System
L-13032	N41° 33' 7.6", W114° 8' 39.2"	NE1/4SE1/4 Sec 4, T42N, R69E
L-13552	N41° 34' 8.1", W114° 8' 2.3"	NW1/4SE1/4 Sec 34, T43N, R69E
L-13553	N41° 34' 8.7", W114° 8' 1.5"	NW1/4SE1/4 Sec 34, T43N, R69E
L-13554	N41° 34' 7.9", W114° 8' 0.7"	NW1/4SE1/4 Sec 34, T43N, R69E
L-13555	N41° 34' 9.3", W114° 8' 1.2"	NW1/4SE1/4 Sec 34, T43N, R69E
L-13556	N41° 34' 8.3", W114° 8' 0.8"	NW1/4SE1/4 Sec 34, T43N, R69E
L-13557	N41° 34' 7.0", W114° 8' 3.9"	NE1/4SW1/4 Sec 34, T43N, R69E
L-13558	N41° 34' 6.8", W114° 8' 6.0"	NE1/4SW1/4 Sec 34, T43N, R69E
L-13559	N41° 34' 6.5", W114° 8' 6.7"	NE1/4SW1/4 Sec 34, T43N, R69E